Universität für Bodenkultur Wien
University of Natural Resources and Life Sciences, Vienna

Department of Biotechnology

Institute of Applied Microbiology

Characterization of Recombinant IgA Producing CHO Cells and Product Purification

Master Thesis

submitted by
Sommeregger Wolfgang, Bakk. techn.
Vienna, April 2012

Supervisor: Kunert Renate, Univ.Prof. Dipl.-Ing. Dr.nat.techn.
Co-Supervisor: Reinhart David, Dipl.-Ing.(FH)

“*If we knew what it was we were doing, it would not be called research, would it?”*
Albert Einstein

Acknowledgements

I deeply thank Prof. Renate Kunert for giving me the opportunity to perform my master thesis at her working group, for advice as well as the exciting discussions.

Further I want to thank David Reinhart for letting me be part of his project, supervision and the great collaboration.

I would further like to thank all the members of the working group, namely Alexander Mader, Bernhard Prewein, Christian Leitner, David Reinhart, David Keiler, Jasmin Peiker, Kathrin Göritzer, Patrick Mayrhofer, Urszula Puc, Stefan Bauernfried, Veronika Chromikova and Willibald Steinfellner for their help and the open-minded creative atmosphere. I enjoyed working with you!

I especially want to thank my family and friends for their incessant support during my studies.

Abstract

Although many techniques are available, the establishment of well-producing recombinant cell lines remains difficult. The two recombinant cell lines 3D6-IgA/5C5 and 4B3-IgA/6H2, that produce IgAs which are both directed against the gp41 envelope protein of the human immunodeficiency virus 1 (HIV-1), were previously generated and resulted in significantly different specific productivities. In this work, we compared the two cell lines according to their IgA heavy chain, light chain and joining chain gene copy numbers as well as the intracellular amount of transcripts. The method of choice for this purpose was quantitative real-time PCR and was performed using genomic DNA and cDNA. Method optimization was conducted and several quantification approaches of real-time PCR were analysed and compared. The obtained results showed differences among the gene copy numbers and also the amount of transcripts. However, no significant correlation between the number of product related gene copies and their transcription rates as well as between the transcription rates and the different specific productivities could be identified. The results suggested that gene copy and transcript numbers are not the only parameters influencing productivities, but bottlenecks elsewhere in the protein expression machinery may control antibody synthesis and secretion. In the second part of this work antibody purification using an IgA affinity matrix was successfully performed with camelid affinity ligands yielding highly pure IgAs with rather good recovery. This down-stream procedure enables IgA purification with high purity and acceptable recovery rates.

Zusammenfassung

Obwohl heutzutage mehrere Techniken zur Verfügung stehen, bleibt die Entwicklung gut produzierender rekombinanter Zelllinien schwierig. Die beiden IgA produzierenden Zelllinien 3D6-IgA/5C5 und 4B3-IgA/6H2, deren Produkte gegen das Hüllprotein gp41 des Humanen Immundefizienz-Virus 1 (HIV-1) gerichtet sind, wurden zuvor entwickelt und zeigten sehr unterschiedliche spezifische Produktionsraten. In der vorgelegten Arbeit wurden die Genkopienzahlen der schweren und leichte Ketten sowie der sogenannten Joining-Chain in beiden Produktionsklonen analysiert und auch die intrazellulären Mengen an Transkripten verglichen. Die Methode der Wahl für diesen Zweck war quantitative Real-time PCR, die für die isolierte genomische DNA und cDNA angewendet wurde. In verschiedenen Vorversuchen wurde die Methode optimiert und anschließend mehrere unabhängige Proben in der Real-time PCR analysiert und verglichen. Die erhaltenen Ergebnisse zeigten Unterschiede zwischen den Gen-Kopienzahlen und auch zwischen der Menge an Transkripten, allerdings konnte keine eindeutige Korrelation zwischen der Anzahl der Genkopien und der Transkriptionsrate sowie zwischen der Transkriptionsrate und den verschiedenen spezifischen Produktivitäten identifiziert werden. Die Ergebnisse legen nahe, dass in diesem Fall Gen-Kopien und Transkriptmengen keinen signifikanten Einfluss auf die Produktivität haben, aber Engpässe in anderen Teilen der Proteinexpressions-Maschinerie die Antikörper-Synthese beeinflussen.

Neben der Bedeutung der Entwicklung gut produzierender Zelllinien für biotechnologische Prozesse besteht auch die Notwendigkeit von funktionellen Methoden zur Reinigung der Produkte, die zu hoher Reinheit und akzeptablen Wiederfindungsraten führen. Im zweiten Teil dieser Arbeit wurden IgA Aufreinigungen mit Hilfe einer IgA Affinitätsmatrix erfolgreich durchgeführt.

Table of Contents

1 Abbreviations 1

2 Introduction 3

3 Project Proposal 5

4 Materials and Methods 7

4.3 Cell Culture 7

4.3.1 Materials and Equipment 7

4.3.2 Cell Line Propagation 8

4.3.3 Cell Counting using Beckmann Coulter Counter 8

4.3.4 Viability 9

4.3.5 Growth Rate: 10

4.3.6 Specific Productivity: 10

4.4 Sandwich ELISA for IgA Quantification 11

4.4.1 Materials and Equipment 11

4.4.2 ELISA 12

4.5 Genomic DNA Isolation 14

4.5.1 Materials and Equipment 14

4.5.2 Isolation 14

4.6 RNA Isolation 16

4.6.1 Materials 16

4.6.2 Isolation 16

4.7 Reverse Transcription 18

4.7.1 Materials and Equipment 18

4.7.2 Method 18

4.8 Primer and Hydrolysis Probes 19

4.9 Polymerase Chain Reaction (PCR) 20

4.9.1 Materials and Equipment 20

4.9.2 PCR 20

4.10 Real-time PCR (qPCR) 21
4.10.1 Materials and Equipment 21
4.10.2 qPCR 21
4.10.3 Quantification Methods 23
4.11 Agarose Gel Electrophoresis 30
4.11.1 Materials and Equipment 30
4.11.2 Method 30
4.12 IgA Purification with Affinity Chromatography 32
4.12.1 Materials and Equipment 32
4.12.2 Chromatography 32
4.13 SDS – PAGE 34
4.13.1 Materials and Equipment 34
4.13.2 Method 34
4.14 Silver Staining of Polyacrylamide Gels 35
4.14.1 Materials and Equipment 35
4.14.2 Staining 35
5 Results 36
5.3 Cell Culture 36
5.3.1 Growth and Productivity over Time 37
5.3.2 Growth Rate and Viability 38
5.3.3 Volumetric Titers 38
5.3.4 Specific Productivity 39
5.4 Gene Copy Analysis 40
5.4.1 Signal Optimization for qPCR 40
5.4.2 Raw Data 41
5.4.3 Quantification 43
5.5 Transcript Copy Analysis 47
5.5.1 Raw Data 47
5.5.2 Quantification 49
5.6 Comparison of gDNA and cDNA Content 52

5.7 Product Purification 53
6 Discussion.....55
6.3 Growth and Productivity 55
6.4 Cell Line Characterization via qPCR 56
6.4.1 Genomic DNA pre-Denaturation improves qPCR Results 56
6.4.2 The Challenge of qPCR Data Interpretation.....56
6.4.3 Gene Copies and Transcript Copies versus Specific Productivity.....58
6.5 Product Purification 59
7 Conclusion 60
8 References.....61

1 Abbreviations

BSA:	Bovine serum albumin
cDNA:	Complementary deoxyribonucleic acid
CHO:	Chinese hamster ovary
Da:	Dalton (= g/mol)
dH_2O:	Deionised water
dIgA:	Dimeric IgA
DMEM:	Dulbecco's modified Eagle's medium
DNA:	Deoxyribonucleic acid
dNTPs:	Deoxy nucleoside triphosphates
ELISA:	Enzyme-linked immunosorbent assay
EtBr:	Ethidium bromide
EtOH:	Ethanol
Gbp:	Giga base - pairs
gDNA:	Genomic DNA
GOI:	Gene of interest
HC:	Heavy chain
HIV:	Human immunodeficiency virus
HT:	Hypoxanthin - Thymidin - supplement
IgA:	Immunoglobulin isotype A
IgG:	Immunoglobulin isotype G
JC:	Joining chain
LC:	Light chain
MTX:	Methotrexat
PAGE:	Poly acrylamide gel electrophoresis
PBS:	Phosphate buffered saline
PCR:	Polymerase chain reaction
RFU:	Relative fluorescence units

rpm:	Rounds per minute
RT:	Room temperature
SDS:	Sodium dodecyl sulfate

2 Introduction

Mammalian cells are nowadays widely used for recombinant protein production because of their ability of proper protein folding, assembly and post translational modifications (*1*). The isolation of dihydrofolate reductase (dhfr) deficient CHO-DUKX-B11 cells by Urlaub and Chasin in the year 1980 was the essential basis for the subsequently extensive use of CHO cells in biotechnology for recombinant protein production until present days (*2*). The dhfr deficiency of the CHO cells is very important for the selection and amplification of transfected cells via hypoxanthine and thymidine (HT) omission in combination with methotrexate (MTX) supplementation .

Today, the reached volumetric yields of recombinantly produced proteins are much higher than in the beginning of mammalian cell culture, but the establishment of well-producing cell lines is difficult and not always successful. Furthermore, similarly generated cell lines that produce similar products are often very diverse in terms of productivity. The factors that are considered to be influential in production diversity are gene copy number, transcription rate, translational efficiency, post translational modifications as well as the protein secretion pathways (*3, 4*).

Bad production yields are a major problem in biotechnological processes and can lead to unprofitable products. Improvement of mammalian protein production is therefore a huge research field and higher yields could be achieved by further developments in production systems through vector and host cell engineering as well as better understanding of molecular and cellular biology (*1*).

In the field of biotechnology not only the upstream process of generating a stable and good producing cell line is crucial, there is also the need of good product purification methods (downstream processing).

The market of biopharmaceuticals is constantly growing and one essential group of these therapeutics are recombinantly produced antibodies (*5*). Naturally mammalian antibodies appear in 5 different isotypes G, M, A, D, E and every isotype fulfils other functions in immunity (*6*). Monoclonal antibodies have a high potential in medical therapies and in the year 2010 7% of the worldwide sold biopharmaceuticals were antibodies (*7*) but none of these antibodies were IgA.isotypes. Though the amount of

IgA in serum is lower compared to IgG, IgA is the predominantly secreted immunoglobulin class and therefore plays an important role in passive (and possibly active) protection of mucosal surfaces against microorganisms and viruses (*8*). Due to the absence of effective therapies against several infections and because mucosal surfaces are the main entrances of pathogens into the body, the idea of using IgAs for passive immunization got in focus (*9*).

Worldwide, human immunodeficiency virus (HIV) infections are still rising and reached an estimated number of 33.4 million infected people in the year 2008 (*10*). Therefore researchers around the world make a huge effort to find ways to prevent the infection or cure the disease.

Two recombinant cell lines 3D6-IgA/5C5 and 4B3-IgA/6H2, which express IgA antibodies directed against the gp41 envelope protein of the human immunodeficiency virus 1 (HIV-1) were previously generated and observed to be substantially different among their specific productivities (*11, 12*).

In this study we investigated the two cell lines according to specific productivities, gene copy and transcript numbers and compared as well as correlated the results. Furthermore, IgA antibodies were purified by affinity chromatography obtaining high yields and purities.

3 Project Proposal

The two recombinant IgA producing cell lines 3D6-IgA/5C5 and 4B3-IgA/6H2 were generated from CHO DUKX-B11 dhfr- cells in the same way (*11, 12*) by co-transfection of three plasmids (Figure 1).

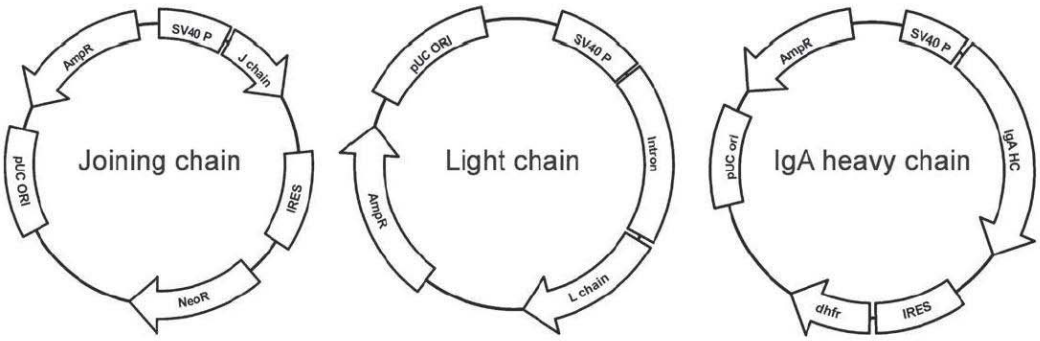

Figure 1:Plasmids used for the co transfection of dhfr- deficient CHO host cell line (*11*).

The established cell lines show a significant difference in specific productivity (*12*), although the only differences among the genetic information were the variable regions of the heavy chain and the whole light chains which were a lambda light chain for 4B3-IgA and a kappa light chain for 3D6-IgA (Figure 2).

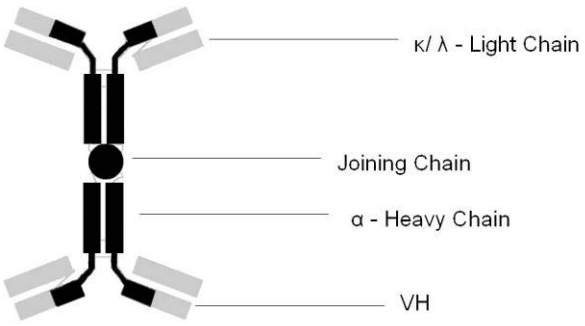

Figure 2: Schematic illustration of a dimeric IgA. Black parts indicate the same genetic information for both recombinant cell lines whereas grey parts are different between 3D6-IgA and 4B3-IgA.

The main goal of this project was to observe the two cell lines over time respective to their growth rates and productivities and to find out if differences among the gene copy numbers or the transcription rates are the cause of the significant variation in specific productivity.

The second part of my work was considered to verify the purification capacity of camelid ligands for IgAs as described by Reinhart et al. .

4 Materials and Methods

4.3 Cell Culture

4.3.1 Materials and Equipment

Table 1: Materials and equipment used in cell culture.

Spinner flasks:	Techne complete culture vessel 125 mL (F7988)
Roux flasks:	Nunc Nunclon ∆ surface T25 flasks (163371)
Cultivation medium:	Biochrom AG DMEM/HAM's F12 (1:1) (F4815) + 4 mM L-glutamine + Protein free supplement (Polymun Scientific) + Soy peptone (Polymun Scientific) + Pluronic F68 + 0.1 mM hypoxanthine, 0.016 mM thymidine (HT)
Amplification medium:	Lonza ProCHO5 w/Pluronic w/o L-Gln or HT (BE12-766Q) + 4 mM L-glutamine + 15 mg/L phenol red + 0.096 µM MTX
Trypan blue staining solution:	0.5% Trypan blue
Particle counter:	Beckmann Coulter Z2 Coulter counter
Cell lysis buffer:	0.1 M citric acid 2% Triton X-100
Counting buffer	Beckmann Coulter isoton II diluent (BCC-8546719)

4.3.2 Cell Line Propagation

All used cell lines grew in suspension and under serum free conditions.

CHO-DUKX-B11 dhfr- host cell line was cultivated in a T25 Roux flask with 10 mL cultivation medium. The Roux flask was kept under 98% humidity at 37 °C in a 7% CO_2 incubator with its cap a half-twist opened. The cells were passaged under sterile conditions to a initial cell density of 2 x 10^5 cells per mL every 3rd to 4th day.

4B3-IgA/6H2 and 3D6-IgA/5C5 cell lines that were generated from CHO-DUKX-B11 dhfr- cells, have been cultivated in CO_2 primed spinner flasks with 40 mL amplification medium containing 0.096 µM MTX. The spinner flasks were kept on a magnetic stirrer (50 rpm) at 37 °C. Every 3 to 4 days the cells were passaged to a cell density of 2.5 x 10^5 cells per mL.

4.3.3 Cell Counting using Beckmann Coulter Counter

To calculate the passage split ratio, growth rate and specific productivity, cell counting was done before each passage using a Beckmann Coulter counter. For this method of cell counting 2 mL of the homogeneous suspension culture were harvested and centrifuged at 190 g for 10 minutes and the supernatant was collected for later productivity analysis. The cell pellet was mixed with 1 mL of cell lysis buffer and incubated for 2 hours at room temperature for proper cell lysis. Afterwards 100 µL of this lysate were added to 9 mL of counting buffer. 0.5 mL of this solution were analysed by the Beckmann Coulter counter.. The number of cells per mL was calculated as follows (Figure 3):

$$Cells\ per\ mL = \frac{counts * total\ volume\,[mL] * 2}{lysate\,[mL] * CF}$$

Figure 3: Formula to calculate the amount of cells per mL , where CF is the concentration factor that is based on the harvested suspension culture and the volume of lysis buffer that is added to the pellet after centrifugation. CF would be “2” if 2 mL of suspension and 1 mL of lysis buffer were used.

Figure 4 shows the size distribution of lysed cells, resulting in free nuclei, counted by Beckmann Coulter counter.

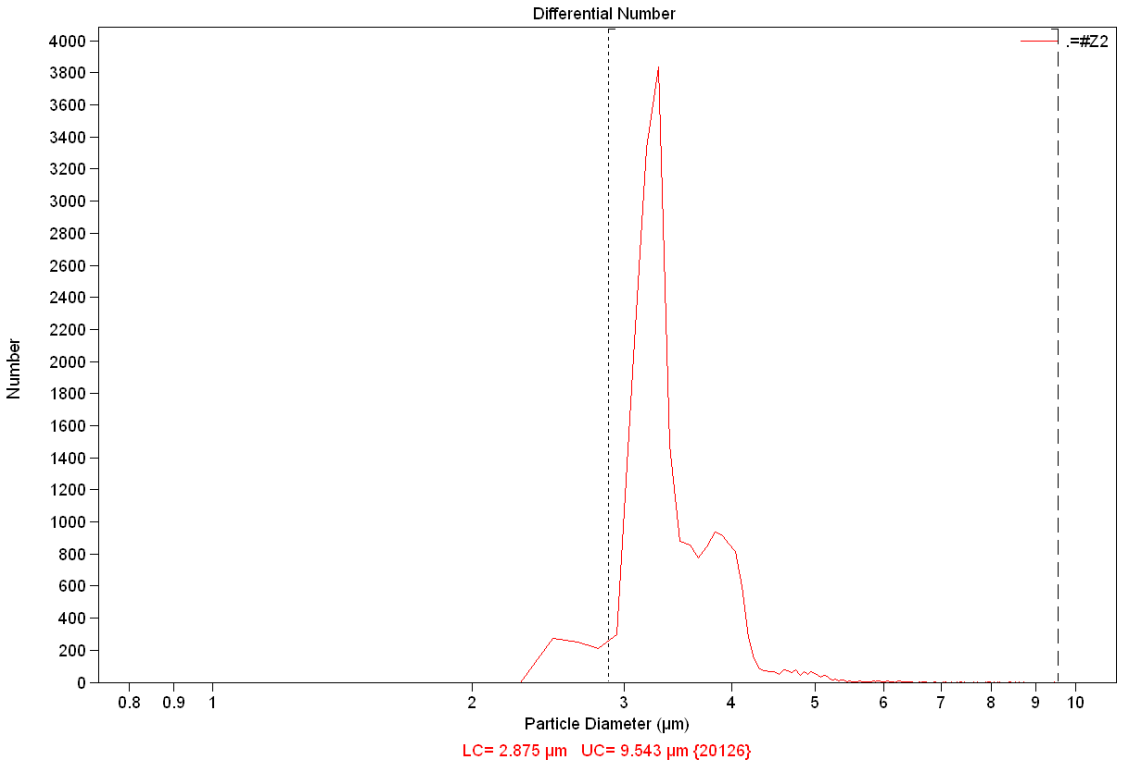

Figure 4: Normal distribution of counted cell nuclei according to their size. In this example particles from 2.875 µm to 9.543 µm were taken into account, representing cells in G1 phase (large peak) and cells in S or G2 phase (small peak). Smaller sized particles were considered to be cell debris and were neglected for the analysis.

4.3.4 Viability

To calculate the percentage of viable cells in the cultures 0.5 mL of the homogeneous suspension culture was harvested and analysed. Dead cells were stained by adding 100 µL of Trypan blue staining solution to the harvested cell suspension and a part of it was then transferred to a haemocytometer and analysed optically by microscopy. Dead cells lose their cell membrane integrity and can be determined by blue colour inclusion. Viability was calculated in the following way (Figure 5):

$$Viability[\%] = \frac{viable\ cells}{total\ cells} * 100$$

Figure 5: Formula to calculate the percentage of viable cells.

4.3.5 Growth Rate:

The growth rate was calculated as follows (Figure 6):

$$Growth\,rate\,\mu\ \left[\frac{1}{d}\right] = \frac{ln(\frac{X_1}{X_0})}{t}$$

Figure 6: Formula to calculate the growth rate per day, where X_1 is the final cell density, X_0 the initial cell density and t is time in days.

4.3.6 Specific Productivity:

The specific productivity was calculated as follows (Figure 7):

$$Specific\ productivity\ qp\ \left[\frac{\mu g}{d * 10^6\ cells}\right] = \frac{P_1 - P_0}{X_1 - X_0} * \mu * 10^6$$

Figure 7: Formula to calculate the specific productivity, where P_1 is the final product titer and P_0 is the starting product titer of each passage.

4.4 Sandwich ELISA for IgA Quantification

4.4.1 Materials and Equipment

Table 2: Materials and equipment used for quantitative ELISA.

Multichannel pipette	Thermo Scientific Finnpipette F2
Coating plate	Nunc Immuno 96 MicroWell plate, MaxiSorp
Dilution plate	Nunc 96 MicroWell plate
Microplate washer	Tecan Microplate Washer 96PW
Microplate reader	Tecan Infinite M1000 pro
Shaker	VWR incubating microplate shaker
Software application:	Magellan V6.6.
10x PBS stock solution (5 L)	57.5 g Na_2HPO_4 * 2 H_2O 10 g KH_2PO_4 10 g KCl 400 g NaCl filled up to a total volume of 5 L with dH_2O
Washing buffer (1x TPBS) (1 L)	100 mL of 10x PBS stock solution 1 mL Tween filled up to a total volume of 1 L with dH_2O
Dilution buffer (100 mL)	100 mL washing buffer 1 g BSA
Coating buffer (1 L)	8,4 g $NaHCO_3$ 4,2 g Na_2CO_3 filled up to a total volume of 1 L with dH_2O pH 9.5 – 9.8
Colouring buffer (1 L)	7.3 g citric acid * H_2O 11.86 g Na_2HPO_4 * 2 H_2O filled up to a total volume of 1 L with dH_2O pH 4.8 – 5.0
OPD	Ortho-phenylenediamine (100 mg/mL)
H_2SO_4	25 % H_2SO_4

4.4.2 ELISA

Coating of 96-well Microplate

100 µL per well of coating antibody (anti-human IgA alpha-chain, Sigma I0884, 1 mg/mL) diluted 1:1000 in coating buffer were transferred to the 96-well plate (Nunc, MaxiSorp) using a multichannel pipette. For antibody binding the plate was incubated for 2 hours on a shaker (300 rpm, RT) or overnight without shaking (4 °C). Afterwards the non-bound antibody was washed off the plate using a plate washer.

Sample and Standard Preparation

Standards and samples were diluted with dilution buffer in a 1:2 dilution series on a dilution plate using a multichannel pipette. Purified 3D6-IgA or 4B3-IgA was adjusted to a concentration of 400 ng/mL and used as standard.

Transfer of Samples from Dilution Plate to the Pre-coated Plate

50 µL of sample were transferred to the pre-coated plate and incubated for 1 hour on a shaker (300 rpm, RT) and afterwards the plate was washed 3 times.

Conjugation with Secondary Antibody

1:1000 diluted anti-human kappa light-chains – Peroxidase (Sigma; A-7164) in dilution buffer was used for the detection of 3D6-IgA and 1:200 diluted anti-human lambda light-chains – Peroxidase (Southern Biotech; 9180-05) in dilution buffer for the detection of 4B3-IgA. 50 µL conjugate per well were transferred to the microtiter plate. The plate was incubated one hour on a shaker (300 rpm, RT) for binding of secondary antibody to the product and afterwards washed to remove unbound antibody using the plate washer.

Colour Reaction and Analysis

The colour reaction was induced by adding 100 µL of colouring buffer including OPD (1%) and H_2O_2 (0.6 µL) to each well and stopped by adding 100 µL H_2SO_4.

The plate was analysed using a plate reader (excitation wave length 492 nm, emission 620 nm) and with the software application Magellan V6.6 quantification relative to the standard curve was done.

4.5 Genomic DNA Isolation

4.5.1 Materials and Equipment

Table 3: Equipment and materials used for genomic DNA isolation.

Photometer:	Implen NanoPhotometer P-300
DNA isolation kit:	QIAGEN QIAamp DNA Blood Mini kit (51106)
1x PBS:	1.15 g $Na_2HPO4 * 2 H_2O$ 0.2 g KH_2PO_4 0.2 g KCl 8 g NaCl filled up to a total volume of 1 L with dH_2O

4.5.2 Isolation

The genomic DNA was isolated from 2 x 10^6 CHO cells using the QIAGEN Blood Mini kit according to the manufacturer's protocol (protocol for cultured cells with RNAse treatment).

Brief summary:

- Cells were harvested, centrifuged, resuspended in PBS (200 µL) and Proteinase K (40 µL) and RNAse A (4 µL) were added.
- Lysis buffer was added, incubated for 10 minutes at 56 °C and afterwards absolute ethanol was added for DNA precipitation.
- The solution was transferred to a QIAmp Mini spin column and centrifuged.
- The DNA bound to the column was washed two times using different buffers and finally eluted in dH_2O.

Solutions and Enzymes except PBS and ethanol were provided with the isolation kit. The DNA concentration was measured photometrically by the absorbance at 260 nm. Purity was controlled by the ratio of absorbance at 260 nm to the absorbance at 280 nm. The ratio of purified DNA lied between 1.7 and 1.9.

$$DNA\ concentration\ [\mu g/mL] = Abs_{260} * 50\ \mu g/mL$$

Figure 8: Formula to calculate the DNA concentration.

The isolated genomic DNA was stored at +4 °C.

4.6 RNA Isolation

4.6.1 Materials

Table 4: Materials used for RNA isolation.

Trizol reagent	Ambion Tri reagent solution (AM9738)
RNase free, DNAse I reaction buffer	QIAGEN RNAse free DNAse set (79254)
RNAse free water	QIAGEN RNAse free DNAse set (79254)
DNAse I	QIAGEN RNAse free DNAse set (79254) (1500 Kunitz units in 550 µL)
RNAse inhibitor	Invitrogen RNAse out ribonuclease inhibitor (40 U/ µL) (10777-019)

4.6.2 Isolation

Cellular RNA was isolated from 5 x 10^6 CHO cells using Trizol:

- 5 x 10^6 cells were lysed by adding 1 mL Trizol reagent, 200 µL chloroform and incubated on ice for 10 minutes.
- The solution was centrifuged at 16,100 g for 15 minutes at +4 °C.
- The aqueous, colourless upper phase was transferred into a fresh centrifugation tube and mixed with 500 µL isopropanol, incubated at -20°C for 15 minutes, centrifuged (16,100 g, 15 min, +4 °C) and the supernatant was discarded.
- The pellet was washed with 1 mL ethanol (70 %), centrifuged (16,100 g, 5 min, +4 °C), supernatant was discarded and the pellet dried at RT.
- The dry pellet was dissolved in 70 µL RNase free, DNAse I reaction buffer and 10 µL DNAse I and 4 µL RNAse Inhibitor were added and incubated at RT for 30 minutes. Afterwards the solution was heated to 75 °C for 10 min to inactivate DNAse I.

- 250 µL Isopropanol were added and incubated at -20 °C for 15 minutes, centrifuged (16,100 g, 15 min, +4 °C) and the supernatant was discarded.
- The pellet was washed with 1 mL ethanol (70 %), centrifuged (16,100 g, 5 min, +4 °C) and dried at RT.
- The pellet was dissolved in 23.5 µl RNase free water + 1.5 µL RNase inhibitor by incubation at RT for 10 minutes.

The RNA concentration was measured photometrically by the absorbance at 260 nm. Purity was checked by the ratio of absorbance at 260 nm to the absorbance at 280 nm.

$$RNA\ concentration\ [\mu g/mL] = Abs_{260} * 40\ \mu g/mL$$

Figure 9: Formula to calculate the RNA concentration.

The isolated RNA was stored at -20 °C.

4.7 Reverse Transcription

4.7.1 Materials and Equipment

Table 5: Materials used for reverse transcription

dNTPs	New England Bilolabs deoxynucleotide solution mix (10 mM each dNTP) (N0447L)
RNase inhibitor	Invitrogen RNAse out ribonuclease inhibitor (40 U/ µL) (10777-019)
Reverse transcriptase buffer (5x)	Promega M-MLV RT 5x buffer (M531A)
Reverse transcriptase (200 U/µL)	Promega M-MLV reverse transcriptase (200 U/µL) (M170A)
Random primers	Promega random primers (500ng/µL) (C1181)

4.7.2 Method

To generate cDNA the isolated RNA was reverse transcribed using random primers and Moloney murine leukaemia virus reverse transcriptase as follows (Table 6) and afterwards stored at +4 °C.

Table 6: Reverse transcription protocol.

RNA	1.5 µg
Random Primers	2 µL
dNTPs	1 µL
dH_2O	to 14 µL
1. 70 °C, 5 min 2. RT, 2 min	
RNase Inhibitor	1 µL
Reverse Transcriptase Buffer	4 µL
Reverse Transcriptase	1 µL
	20 µL
1. 37 °C, 30 min 2. 95 °C, 5 min	

4.8 Primer and Hydrolysis Probes

Primer and hydrolysis probes have been designed using the Primer 3 web application (http://frodo.wi.mit.edu/primer3/, 03/29/2012, version 4.0) (*11, 13*). Secondary structures were controlled with the web application OligoCalc (http://www.basic.northwestern.edu/biotools/oligocalc.html, 03/29/2012, version 3.26) (*14*).

Table 7: List of used primers and hydrolysis probes.

Heavy chain sense primer:	AGTCCAAGACCCCTCTGACC	Amplicon size 199 bp
Heavy chain antisense primer:	TACTTCTCCCGAGGCAGTTC	
Heavy chain hydrolysis probe:	**[6FAM]**CCGGCAACACCTTCAGACCTGA**[TAM]**	
Joining chain sense primer:	CTCTGAACAACCGGGAGAAC	Amplicon size 194 bp
Joining chain antisense primer:	GTTCCGGTCGTAGGTGTAGC	
Joining chain hydrolysis probe:	**[6FAM]**CACCTGTCCGACCTGTGCAAGAA**[TAM]**	
4B3 light chain sense primer:	TCTGCCTGATCTCCGACTTC	Amplicon size 186 bp
4B3 light chain antisense primer :	CCTGGCAAGAGTAGGACCTG	
4B3 light chain hydrolysis probe:	**[6FAM]**CCCTTCCAAGCAGTCCAACAACAAG**[TAM]**	
3D6 light chain sense primer:	TGTGCCTGCTGAACAACTTC	Amplicon size 183 bp
3D6 light chain antisense primer:	AGGCGTACACCTTGTGCTTC	
3D6 light chain hydrolysis probe:	**[6FAM]**AGCAGCACCCTGACCCTGTCCAA**[TAM]**	
ß-actin sense primer:	TGAGCGCAAGTACTCTGTG	Amplicon size 78 bp
ß-actin antisense primer:	TTGCTGATCCACATCTCCTG	
ß-actin hydrolysis probe:	**[6FAM]**CCATCCTGGCCTCACTGTCCACCT**[TAM]**	

All primers and probes were synthesized by Sigma-Aldrich.

4.9 Polymerase Chain Reaction (PCR)

4.9.1 Materials and Equipment

Table 8: Materials and equipment used for PCR.

Supermix (2x):	BioRad iQ Supermix (1708860)
Thermocycler:	BioRad C1000 thermal cycler

4.9.2 PCR

DNA target amplification was done with PCR as follows:

PCR Reaction Mix:

Table 9: PCR Reaction Mix.

IQ supermix:	10 µL
Primer s:	6 pmol
Primer as:	6 pmol
dH_2O:	x µL
Template:	x µL
Final reaction volume:	20 µL

PCR-Conditions

1. Initial denaturation	95 °C (5 min)
2. Annealing and extension:	55 °C (60 sec)
3. Denaturation:	95 °C (15 sec)

Step 2 and 3 were repeated 39 times.

4.10 Real-time PCR (qPCR)

4.10.1 Materials and Equipment

Table 10: Materials and equipment used for Real-time PCR.

Supermix (2x):	BioRad iQ supermix (1708860)
Real-time PCR machine:	BioRad MiniOpticon
Software applications:	BioRad CFX Manager LinReg (Version 12.17) (http://LinRegPCR.nl, 03/29/2012) (*15*), (*16*), (*17*) Camper (Version 1.2) (http://www.cebitec.uni-bielefeld.de/groups/brf/software/camper_info/, 03/29/2012) using the FPLM – method (*18*)
PCR plates:	BioRad Multiplate PCR plates, low 48-well white (MLL4851)
PCR plate sealer:	BioRad PCR Sealers, Microseal B film (MSB1001)

4.10.2 qPCR

To quantify the amount of (ß-actin), heavy chain, joining chain and light chain DNA in the genome as well as the amount of transcript of the two cell lines 4B3-IgA/6H2 and 3D6-IgA/5C5, qPCR was performed using the designed primers and hydrolysis probes listed above.

Hydrolysis probes release a fluorophor when they are cleaved by the exonuclease activity of the polymerase while the elongation takes place and at each cycle of

amplification the fluorescence signal increases exponentially. The increase of fluorescence was detected by the real-time PCR machine (BioRad MiniOpticon).

Genomic template DNA was isolated using the Blood Mini kit as described before and heated to 99 °C for 10 minutes for proper denaturation prior to qPCR.

The mRNA was isolated and reverse transcribed to cDNA as described in section 4.6 and a 1:50 dilution was directly used for the real-time PCR.

The amount of template DNA for the qPCR of genomic DNA was 3 ng per reaction whereas template cDNA was not quantified before usage. CHO-K1 cell line is known to have a genomic size of 2.45 Gbp DNA (*19*). The genomic size of CHO–DUKX–B11 is not known yet but assumed to be similar. With an average molecular weight of 660 Da per bp and assuming the genomic size of K1, the genomic DNA content of one CHO–DUKX-B11 cell was calculated to be approximately 2.7 pg (Figure 10). The applied 3 ng genomic DNA per reaction would therefore represent roughly 1100 cells.

$$DNA\ content\ per\ cell = 2.45 * 10^9[bp] * 660[g/mol]/(6.022 * 10^{23}[mol]) * 10^{12} = 2.7[pg]$$

Figure 10: Equation to calculate the genomic DNA content of one CHO-DUKX-B11 cell.

The qPCR was performed with each reaction mix in triplicate using three different isolation replicates of each recombinant cell line (biological replicates). At each qPCR run negative controls (NC) and no template controls (NTC) as well as no reverse transcriptase controls (NRT) for the analysis of transcripts were included. Every qPCR was performed in duplicate (technical replicates) as follows:

qPCR Reaction Mixes:

Table 11: qPCR reaction mixes.

Heavy Chain, Joining Chain, ß-actin:

iQ supermix:	10 µL
Primer s:	6 pmol
Primer as:	6 pmol
Probe:	4 pmol
dH_2O:	x µL
Template:	x µL
Final reaction volume:	20 µL

Light Chains:

iQ supermix:	10 µL
Primer s:	12 pmol
Primer as:	12 pmol
Probe:	8 pmol
dH_2O:	x µL
Template:	x µL
Final reaction volume:	20 µL

Each reaction mix was carefully transferred to the qPCR plate to avoid cross contaminations. Afterwards the plate was sealed and the qPCR was started using the following settings:

qPCR-Conditions:

1. Initial Denaturation 95 °C (5 min)
2. Annealing and Extension: 55 °C (60 sec)
3. Fluorescence Detection
4. Denaturation: 95 °C (15 sec)

Step 2 - 4 were repeated 39 times

4.10.3 Quantification Methods

Theoretical Background

The fluorescence of the reaction mix increases with every amplification step. The take-off cycle of the fluorescence curve is called Cq–value (cycle for quantification) (Figure 11) and was calculated by the BioRad CFX Manager by linear regression and baseline subtraction.

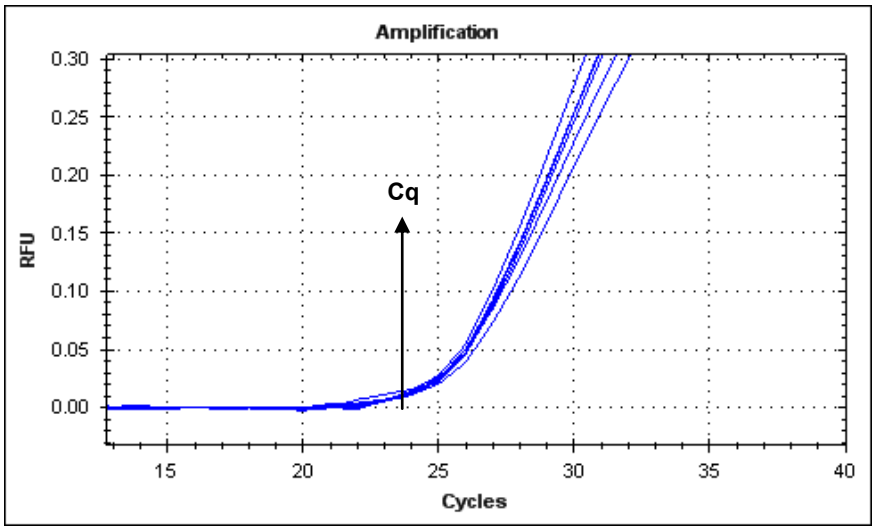

Figure 11: Enlarged graph of relative fluorescence plotted against the qPCR cycle.

In literature this value is also referred to as Ct (cycle threshold) or Cp (crossing point). However, in this work always the term Cq is used according to the MIQE guidelines (*20*).

Results of the real time PCR method can either be described in an absolute manner or relatively to a reference gene. In case of absolute quantification the sample is compared to a standard curve in which the standard not always is derived from the same origin like the sample. The relative quantification describes the gene copy number of a gene of interest according to an internal reference gene. The relative quantification approach is nowadays the most popular method to determine differences between samples (*20*).

In this work the raw data of real time PCR were analysed using different relative quantification approaches (with and without efficiency correction).

To describe the deviations of result we calculated the errors by the law of propagation of uncertainty according to Doerffel (*21*) (Figure 12).

$$Z = X * Y \text{ or } Z = X/Y \longrightarrow \left(\frac{\sigma_Z}{Z}\right)^2 = \left(\frac{\sigma_X}{X}\right)^2 * \left(\frac{\sigma_Y}{Y}\right)^2$$

Figure 12: Error propagation according to Doerffel. If you have an equation like one of the two on the left side the error would be calculated with the formula on the right site, where δ indicates the standard deviation of the variable.

The used quantification and efficiency calculation approaches are described below.

Relative Quantification ($2^{-\Delta\Delta Cq}$) Method)

For relative quantification an internal reference gene, ß-actin, was measured additionally to the exogenes for each sample. This method is used to express the differences between the gene of interest and the reference gene but it can also be used to compare two different samples (*22*). The easiest way is to assume that during every PCR cycle the number of amplicons is doubled. The calculation of this "100% method" is only based on the differences of the Cq values between the gene of interest and the reference gene (delta Cq values). Figure 13 shows sample and reference specific fluorescence curves and the associated delta Cq values to illustrate the principle of relative quantification.

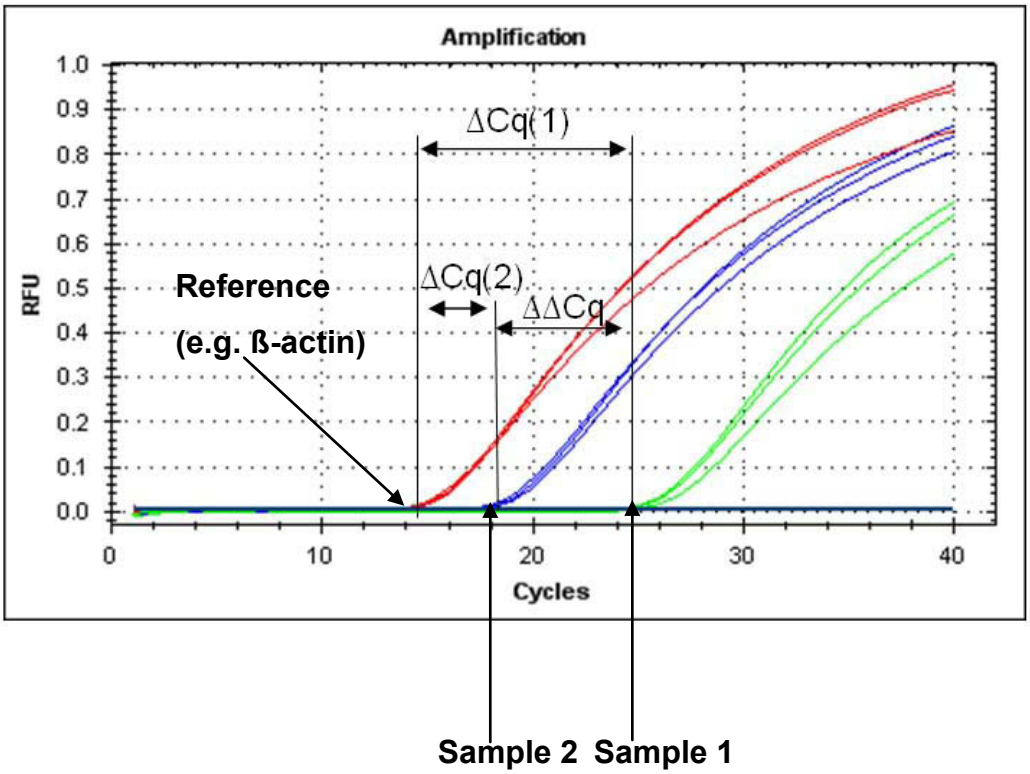

Figure 13: Example of different sample Cqs to illustrate the principle of the Relative Quantification.

The relative Gene copy number is called “ratio” and describes the relation of the gene of interest to the reference gene in the same sample (Figure 14):

$$ratio_{sample\,1} = 2^{-\triangle Cq}$$

$$ratio_{sample\,2} = 2^{-\triangle Cq}$$

Figure 14: Formulas to obtain the relative gene copy numbers.

With this method it is also possible to determine the ratio between two different samples (Figure 15):

$$ratio = 2^{-\triangle\triangle Cq}$$

Figure 15: Formula to express the relation of two genes in two different samples.

The value 2 indicates a doubling at each amplification cycle, which means that this quantification method assumes 100 % real-time PCR efficiency.

When 100% target doubling occurs at each cycle the ΔCq value of a 1:10 dilution of a sample and the undiluted sample would theoretically be 3.32 as illustrated in the following equation (Figure 16):

$$2^{\triangle Cq} = 10 \longrightarrow \triangle Cq = 2log(10) \longrightarrow \triangle Cq = 3.32$$

Figure 16: Equation to show connection between efficiency and the ΔCq value of a 1/10 dilution series.

In practice a 1/10 dilution does not always lead to a ΔCq value of 3.32 because it is not always possible to achieve 100% real-time PCR efficiency and therefore quantification strategies that take the altered efficiency into account came up and are described in the next chapter.

Relative Quantification (with Efficiency Correction)

The relative quantification method with efficiency correction is also known as Pfaffl-method and works similar to the $2^{-\Delta\Delta Cq}$ method but it additionally takes the qPCR efficiency into account (*23*). Figure 17 shows the formula derivations used for

quantification with efficiency correction. The first formula describes the ratio between one sample and the internal reference. The second derivation is used to calculate the ratio between two samples.

$$ratio = (E_{target})^{Cq_{target}(control-sample)}$$

$$ratio = \frac{(E_{target})^{Cq_{target}(control-sample)}}{(E_{ref})^{Cq_{ref}(control-sample)}}$$

Figure 17: Pfaffl – method formula derivations: The first formula describes the relation between a sample and the internal control. The second equation describes the relation between two samples that are both related to the same reference gene.

During the PCR the number of amplicons in the reaction mixture should be doubled, indicated by 100% efficiency (E%). This 100 % efficiency would give the number 2 for a doubling at each cycle. 95% efficiency would give a number of 1.95 (E = 1+E%). In the following table an example of the influence of efficiency correction is shown, if the obtained -ΔCq value is 4 and the true efficiency is 95% instead of 100% the calculated relative gene copies have a percental deviation of 10.7%.

Table 12: Influence of efficiency correction.

obtained -ΔCq value	Efficiency	E	Ratio = $(E)^{-\Delta Cq}$
4.0	100.0%	2.00	16.0
4.0	95.0%	1.95	14.5

percental deviation		
0.0%	5.0%	10.7%

This example makes clear that the qPCR efficiencies (E) influence the quantification significantly and only small variation in efficiency have a significant impact on the final result.

Efficiency Calculation

Several methods exist which are used to calculate the real-time PCR efficiency. Mainly the 1/10 dilution method is used but there are also some mathematical

models available that can be used to calculate the efficiency just out of the fluorescence from a single curve (*24*).

In this project the 1/10 dilution method and the two software applications LinReg and Camper were used to calculate the efficiencies and to compare the different methods according to the results.

The principle of the 1/10 method is attributable to the fact that if a target doubling occurs at each cycle the ΔCq value between two 1:10 dilutions of a sample would theoretically be 3.32 as shown in Figure 16.

By plotting the Cq values of the 1/10 dilution series against the logarithmically scaled concentrations of the template, the slope of the generated curve gives the mean -ΔCq value of the dilution series (see Figure 18). This value is used to calculate the efficiency (see Figure 19). The slope of the curve is therefore directly correlated to the qPCR efficiency; the steeper the curve the lower the efficiency of the PCR.

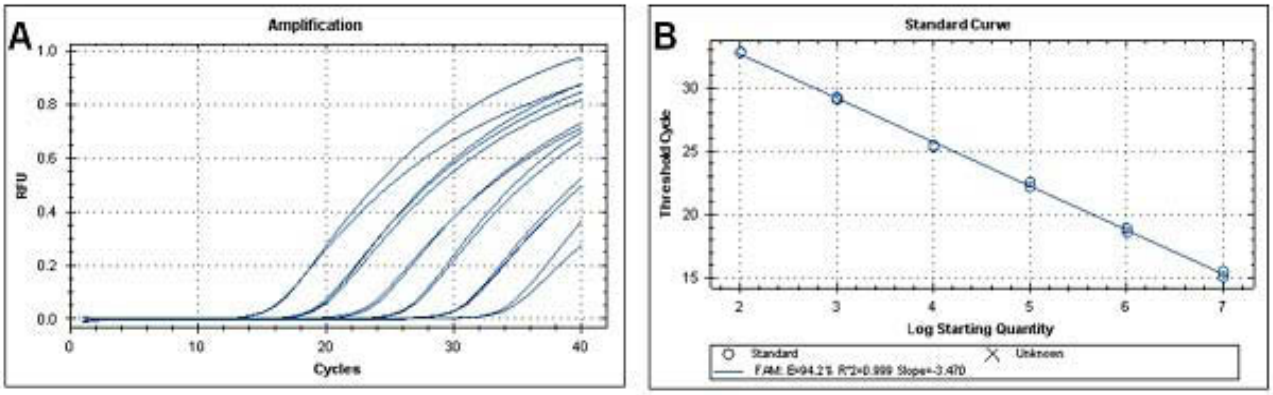

Figure 18: In A the raw fluorescence curves of a 1/10 dilution series are depicted. In B the obtained Cq values are plotted against the logarithmic scaled concentrations to obtain the mean -ΔCq value.

$$E = 10^{(-1/slope)}$$

Figure 19: Formula to calculate the efficiency out of a 1/10 dilution series.

The detailed mathematical algorithms which are used by the chosen software applications LinReg (http://LinRegPCR.nl, 03/29/2012) and Camper (http://www.cebitec.uni-bielefeld.de/groups/brf/software/camper_info/, 03/29/2012) are described elsewhere (*15, 16, 18*). In principle both applications calculate

efficiencies from the single fluorescence curves in the exponential phase via linear regression (LinReg) or an exponential model (Camper).

In literature different approaches are recommended to calculate the qPCR efficiency; either by the means of the calibration curve if the 1/10 method is used (*20*) or different software applications are suggested.

For all efficiency calculation methods applied in this project we calculated mean efficiency values for each amplicon group and used them for further calculations.

4.11 Agarose Gel Electrophoresis

4.11.1 Materials and Equipment

Table 13: Materials and equipment used for agarose gel electrophoresis.

TAE buffer (50x)	242 g Tris Base (MW=121.1 g/MOL) 57.1 mL Glacial Acetic Acid 100 mL 0.5 M EDTA filled up to a total volume of 1 L with dH_2O
Agarose	peqlab peqGOLD universal agarose (35-1020)
Electrophoresis Chamber	BioRad
Power Supply	BioRad Power Pac Basic
Analyser	BioRad Gel Doc XR

4.11.2 Method

Agarose gel electrophoresis was performed to separate DNA by its length.

1% Agarose Gel preparation:

Table 14: 1% Agarose gel preparation.

50x TAE	8 mL
Agarose	4 g
dH_2O	388 mL
Final volume:	400 mL

The solution was boiled in a microwave oven to melt the agarose. The liquid gel was afterwards cooled down to a temperature of approximately 65 °C and 12 µL EtBr were added. The mixture was then poured into gel casting trays with inserted combs. After 30 minutes the polymerized gels were ready to use.

Electrophoresis and Analysis:

The prepared gel was put into an electrophoresis chamber that was filled with 1x TAE buffer and samples were transferred to the pockets of the gel. Electrophoretic separation of samples was conducted at 130 V for 45 min. The gel was then analysed with the BioRad Gel Doc XR.

4.12 IgA Purification with Affinity Chromatography

4.12.1 Materials and Equipment

Table 15: Materials and equipment used for IgA purification with affinity chromatography.

Purifier	ÄKTA purifier
Gel Type:	Capture Select human IgA affinity matrix (BAC, Cat# 2880, Lot# 291008-03) Stored in 20 % EtOH
Equilibration Buffer	PBS, pH 7.4
Elution Buffer	0.1 M Glycine, pH 2.0
Neutralisation Buffer	1 M Tris, pH 9.5
Column	Tricorn 5/100

4.12.2 Chromatography

Affinity chromatography was used for the purification of secreted IgA.

Protocol based on previous research (*11*):

Culture supernatants were concentrated before purification via ultra-/diafiltration to reduce the volume to be loaded on the column.

The column was loaded with affinity matrix and connected to an Äkta chromatography system. The column was washed with equilibration buffer to remove residual ethanol and to equilibrate the affinity matrix until the absorbance at 280 nm of the flow-through was constant (flow rate 1 mL/min). The cell culture supernatant was then loaded onto the column with a flow rate of 0.5 mL per minute. IgA bound to the column and the flow-through was discarded. Afterwards the column was washed

with equilibration buffer until the absorbance at 280 nm of the flow-through was constant. Bound product was then eluted with elution buffer at a flow rate of 0.5 mL/min and immediately pH-neutralised by the addition of neutralisation buffer. The column was washed after its use with equilibration buffer and stored in 20 % ethanol.

After chromatography the different fractions were analysed with quantitative ELISA (see section 4.4) and SDS-PAGE (see section 4.13) to calculate the purification yield.

4.13 SDS – PAGE

4.13.1 Materials and Equipment

Table 16: Materials and equipment used for SDS – PAGE.

Gel:	NuPAGE Novex 3-8% Tris-acetate gel
Tris-Acetate running buffer :	50 mM Tricine 50 mM Tris base 0.1 % SDS pH 8.2
Sample buffer:	NuPage LDS sample buffer (4x) (NP0008)
Power supply:	Invitrogen Power Ease 500
Electrophoresis chamber:	Invitrogen X-Cell Sure Lock
Molecular weight marker:	Invitrogen HiMark pre-stained HMW protein standard (LC5699)

4.13.2 Method

Polyacrylamide gel electrophoresis was performed for the analysis of product purity:

7.5 µL of the sample were mixed with 2.5 µL sample buffer. The ready to use gel cassette was unpacked and put into the electrophoresis chamber that was filled with 1x running buffer. Samples and 10 µL molecular weight marker were transferred into the gel pockets and the gel was run for 1 hour at 150 V. Afterwards the gel was analysed by silver staining (see section 4.14).

4.14 Silver Staining of Polyacrylamide Gels

4.14.1 Materials and Equipment

Table 17: Solutions used for the silver staining of Poly Acrylamide gels.

Fixation solution:	50 % ethanol / 10 % acetic acid in H_2O
Incubation solution:	150 mL ethanol 1.75 g $Na_2S_2O_3$*5H_2O (sodiumthiosulfate pentahydrate) 56.4 g Na-acetate*3H_2O filled up to 500 mL with H_2O + freshly added 62.5 µL glutaraldehyd / 25 mL
Silver solution:	0.25 g $AgNO_3$ in 500 mL H_2O + freshly added 5 µL formaldehyde / 25 mL
Develop solution:	12.5 g Na_2CO_3 in 500 mL H_2O + freshly added 5 µL formaldehyde / 25 mL)
Stop solution:	0.05 M EDTA in H_2O

4.14.2 Staining

The gel was fixed at least 1h in 25 mL fixation solution, afterwards incubated for 20 minutes in 25 mL incubation solution and then washed 3 x 5 minutes in H_2O. The gel was stained with 25 mL silver solution for 15 minutes, briefly washed with water and developed until bands occurred in develop solution. The coloring reaction was stopped by adding stop solution and incubation for 15 minutes – 1 h.

The colored gel was then scanned and analysed.

5 Results

5.3 Cell Culture

The recombinant IgA producing cell lines 3D6-IgA/5C5 and 4B3-IgA/6H2 had been taken over on 2012/09/05 and were propagated for 41 passages. The host cell line CHO–DUKX-B11 dhfr- was propagated for more than 45 passages as control. 3D6-IgA/5C5 was analysed starting from passage 14, 4B3-IgA/6H2 from passage 13, whereas the host cell line was in passage 40. Figure 20 shows pictures of the recombinant suspension cells under a light microscope. The cells are round and homogeneous in size and shape and look viable.

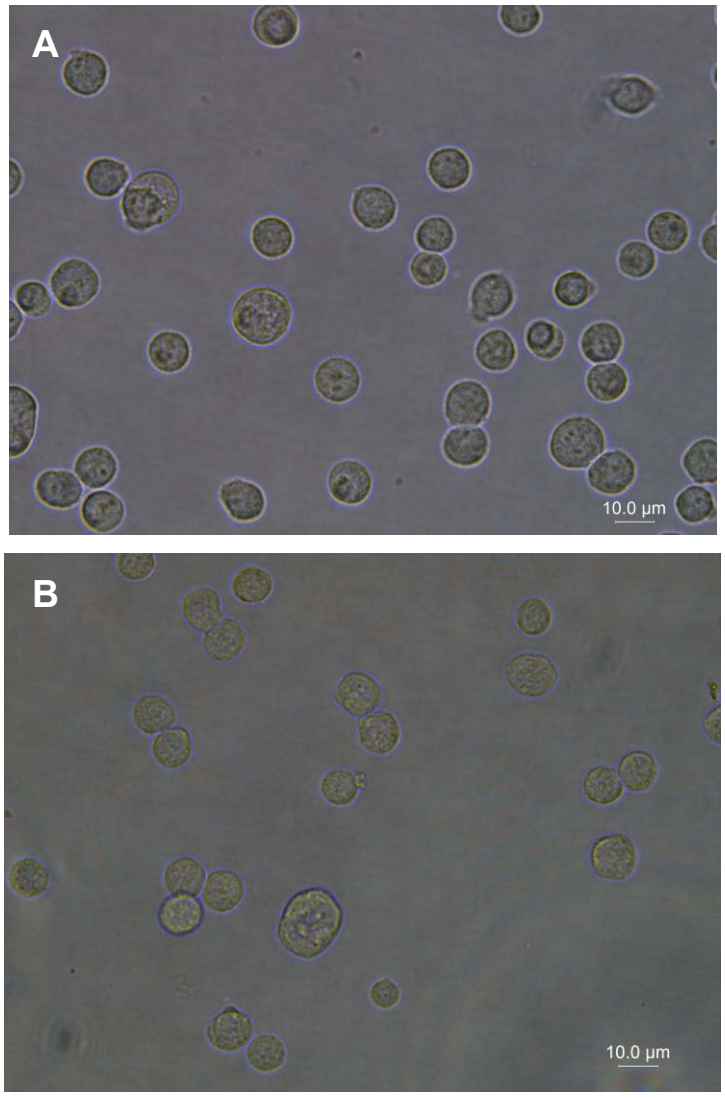

Figure 20: Image of recombinant 4B3-IgA/6H2 (A) and 3D6-IgA/5C5 (B) CHO cell lines under the light microscope.

5.3.1 Growth and Productivity over Time

In Figure 21 growth rate and specific productivity of 4B3-IgA/6H2 are shown. The productivity of clone 4B3-IgA/6H2 dropped substantially from passage 48 towards the end of propagation while the growth rate increased. The timeframe in which the cell line was considered to be stably producing was till passage number 48 and accordingly we calculated mean µ, qp and volumetric titers.

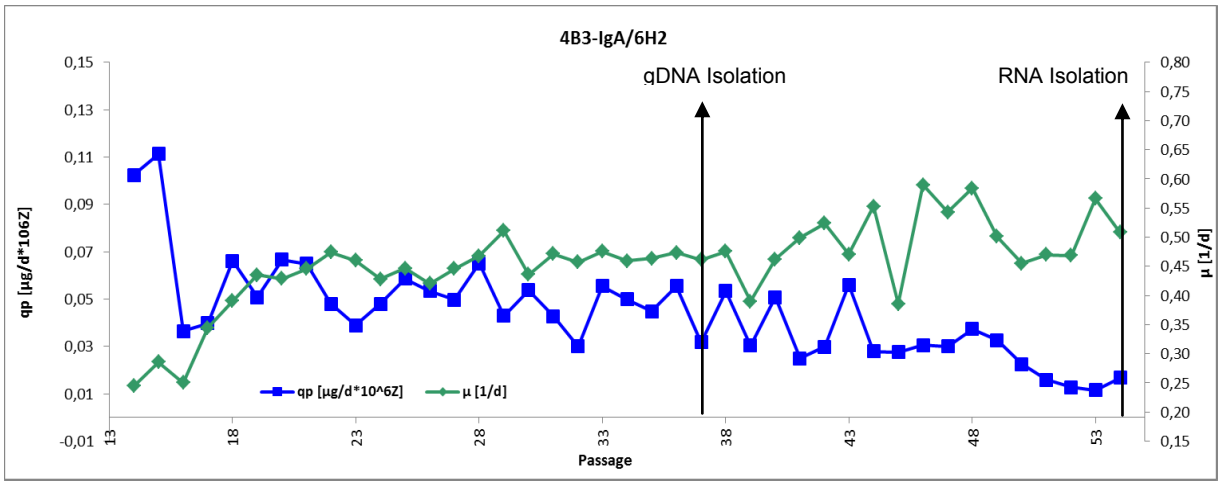

Figure 21: Growth rate µ and specific productivity qp of 4B3-IgA/6H2 plotted over passages.

In Figure 22 growth rate and specific productivity of 3D6-IgA/5C5 are shown. Both, growth rate and productivity slightly increased over the whole propagation period. 3D6–IgA/5C5 was therefore considered to be a stable producing cell line over the whole propagation time.

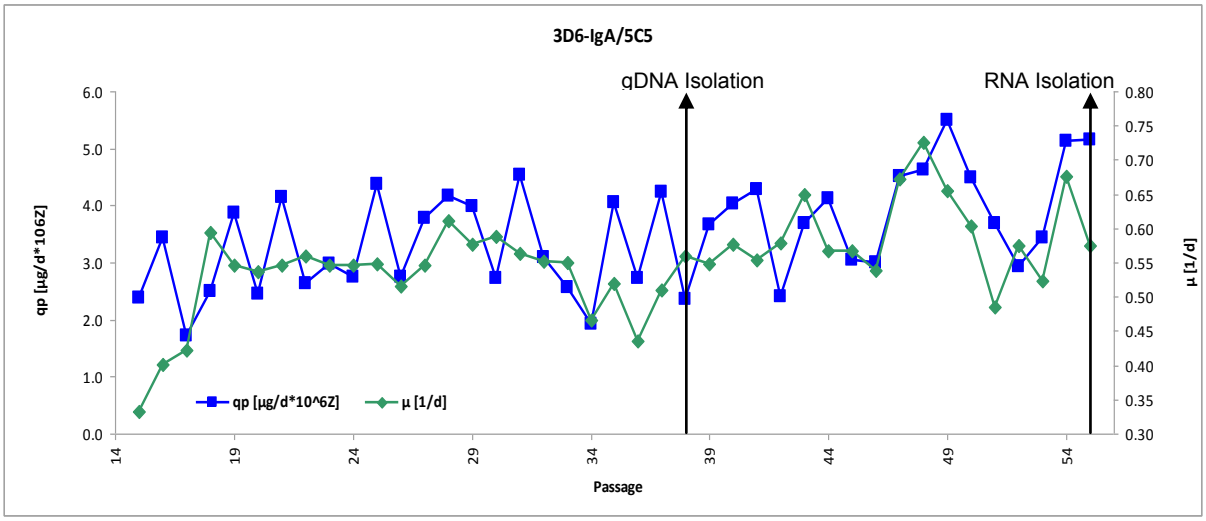

Figure 22: Growth rate µ and specific productivity qp of 3D6-IgA/5C5 plotted over passages.

5.3.2 Growth Rate and Viability

The viability was constantly high in the range of 94 - 100 % for all of the cultivated cell lines over the whole propagation time. Mean growth rates were calculated over all constant passages in culture (see Figure 23), for 4B3-IgA/6H2 the mean was calculated from passage 13 to passage 48 whereas the means for the other two cell lines were calculated over the whole propagation time.

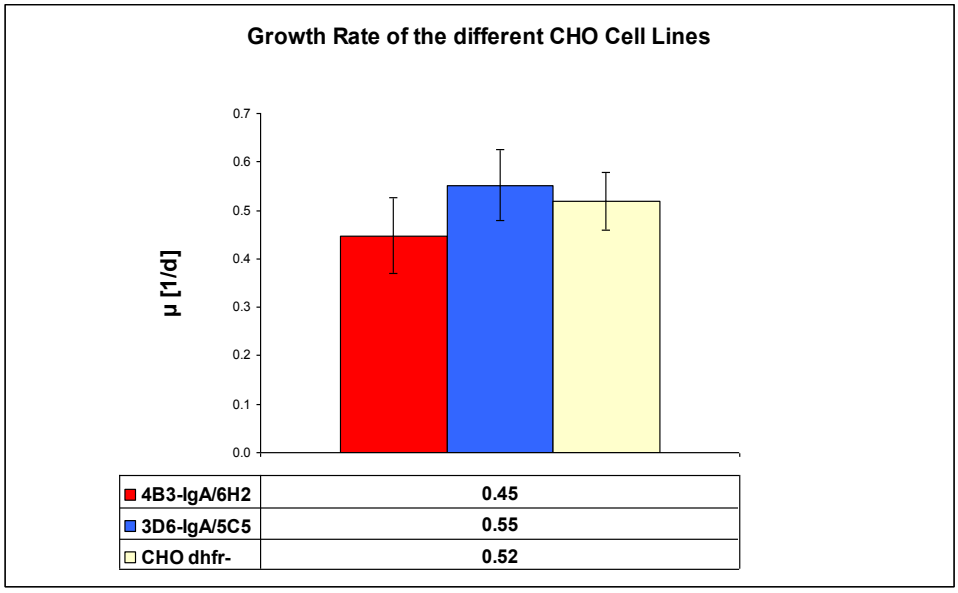

Figure 23: Mean growth rates over the constant passages of the cultivated CHO cell lines.

5.3.3 Volumetric Titers

Volumetric IgA titers were measured by quantitative ELISA at each passage. The mean volumetric titer of the 4B3-IgA/6H2 cell line was calculated till passage 48 whereas the mean for 3D6-IgA/5C5 was calculated over the whole propagation time. The mean titers plotted against a logarithmic scale are shown below Figure 24:

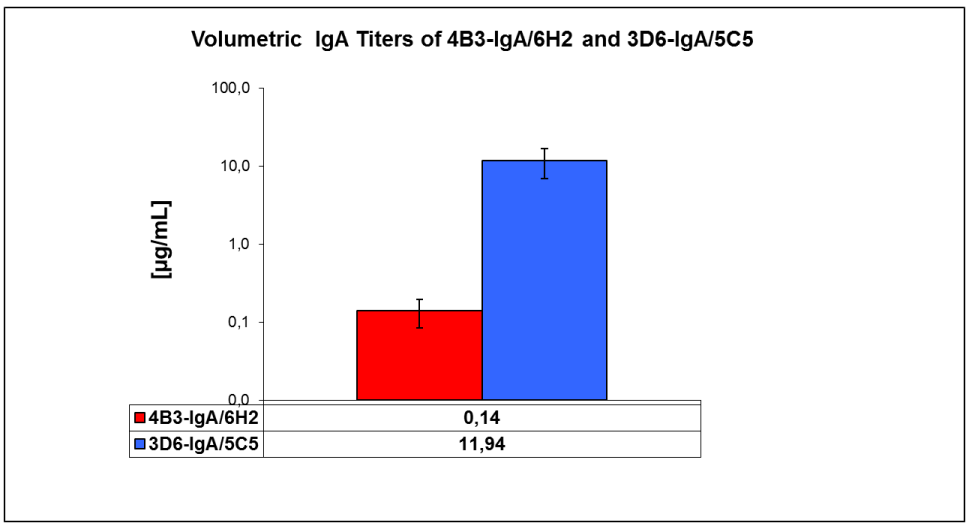

Figure 24: Mean volumetric titers over the constant passages on a logarithmic scale.

5.3.4 Specific Productivity

The volumetric IgA titers that were measured at each passage were used to calculate specific productivities accordingly. The mean values are shown in Figure 25.

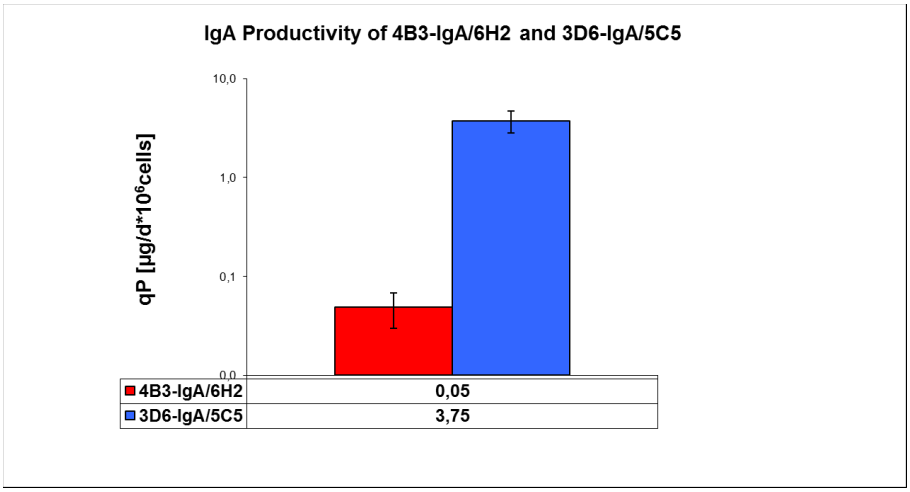

Figure 25: Mean specific productivities of clones 3D6-IgA/5C5 and 4B3-IgA/6H2 over the constant passages on a logarithmic scale.

5.4 Gene Copy Analysis

To determine the relative amount of heavy chain, joining chain and light chain in relation to ß-actin in the genome of the recombinant cell lines qPCR was performed using 3 ng template DNA in each reaction.

The primers were tested in a conventional PCR before using them in real-time PCR. Specific amplicons with the correct size could be determined for all primer pairs in an agarose gel electrophoresis (data not shown).

5.4.1 Signal Optimization for qPCR

The first qPCRs were done without a pre-denaturation step after isolation of genomic DNA which resulted in data with high background noise. Therefore, the protocol was modified to the current including a 10 min denaturation step at 99 °C before qPCR. The improvement of an additional denaturation step is visualized in Figure 26. This improvement in resolution resulted in higher ΔCq (from 1.3 to 2.3) and a decrease in the standard deviation from 0.8 to 0.3 cycles.

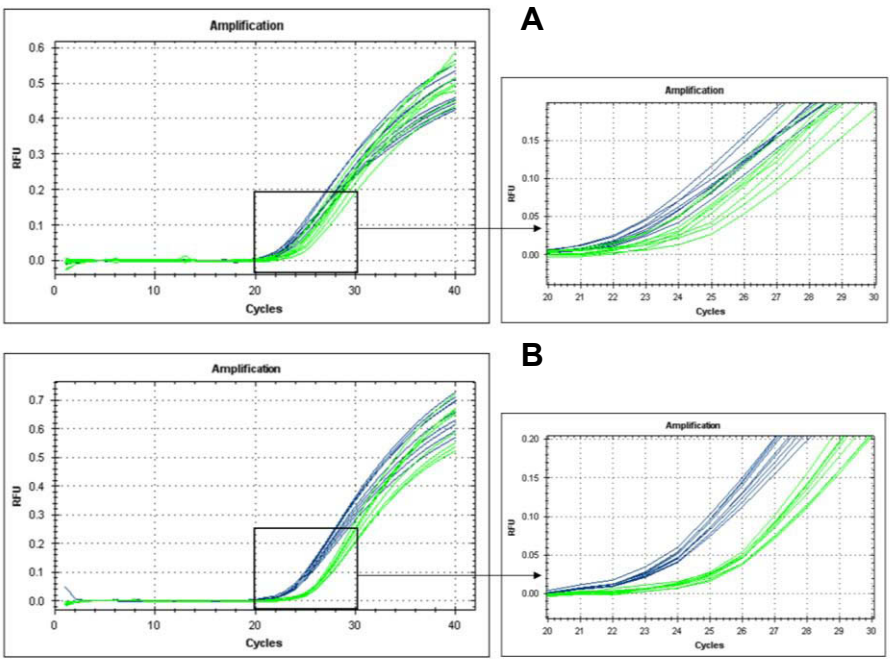

Figure 26: Improvement of Cq distribution by genomic DNA pre-denaturation before the use in qPCR. The same two samples (green and blue) were run in 9 replicates each once without pre-denaturation (A) and once pre-denatured (99 °C, 10min) (B).

5.4.2 Raw Data

The genomic DNA, isolated from the different cell lines was analysed with real-time PCR as described in the methods part. The individual Cq values of each gene of interest in various samples were analysed using the $2^{-\Delta\Delta Cq}$ method and the Pfaffl – method. The mean efficiencies for the Pfaffl – method were calculated with the 1/10 dilution method as well as mathematical algorithms using the LinReg and Camper software applications. The 1/10 dilution method is based on the steepness of a standard curve, generated from Cq values obtained by a 1/10 dilution series plotted against the logarithmic scaled concentrations. In contrast, the two software applications LinReg and Camper calculate the efficiency directly from the raw fluorescence sample curves.

The mean Cq values, ΔCq values and the differently calculated efficiencies, of the triplicates measured in two PCR runs for each GOI of all DNA isolations, are listed in Table 18:

Table 18: Table summarizes the Cq raw data, ΔCq-Values and efficiencies generated by different methods from the three biological replicates of the two production clones.

ß - actin						
DNA Isolate	**Parameter**	**Cq-Value**	**ΔCq-Value**	**Efficiency 1/10**	**Efficiency LinReg**	**Efficiency Camper**
4B3dIgA6H2a	**Mean:**	**24.30**	**Reference**	**1.96**	**2.07**	**1.97**
	Std. Dev.:	*0.12*				
4B3dIgA6H2b	**Mean:**	**24.24**				
	Std. Dev.:	*0.14*				
4B3dIgA6H2c	**Mean:**	**24.11**				
	Std. Dev.:	*0.13*				
3D6dIgA5C5a	**Mean:**	**24.65**	**Reference**			
	Std. Dev.:	*0.17*				
3D6dIgA5C5b	**Mean:**	**24.53**				
	Std. Dev.:	*0.10*				
3D6dIgA5C5c	**Mean:**	**24.60**				
	Std. Dev.:	*0.20*				

Heavy Chain

DNA Isolate	Parameter	Cq-Value	ΔCq-Value	Efficiency 1/10	Efficiency LinReg	Efficiency Camper
4B3dIgA6H2a	**Mean:**	**21.97**	**-2.11**	**1.92**	**1.95**	**1.90**
	Std. Dev.:	*0.05*				
4B3dIgA6H2b	**Mean:**	**22.07**				
	Std. Dev.:	*0.07*				
4B3dIgA6H2c	**Mean:**	**22.29**				
	Std. Dev.:	*0.14*				
3D6dIgA5C5a	**Mean:**	**23.82**	**-1.03**			
	Std. Dev.:	*0.12*				
3D6dIgA5C5b	**Mean:**	**23.26**				
	Std. Dev.:	*0.12*				
3D6dIgA5C5c	**Mean:**	**23.44**				
	Std. Dev.:	*0.16*				

Joining Chain

DNA Isolate	Parameter	Cq-Value	ΔCq-Value	Efficiency 1/10	Efficiency LinReg	Efficiency Camper
4B3dIgA6H2a	**Mean:**	**22.80**	**-1.44**	**1.94**	**1.95**	**1.90**
	Std. Dev.:	*0.05*				
4B3dIgA6H2b	**Mean:**	**22.81**				
	Std. Dev.:	*0.07*				
4B3dIgA6H2c	**Mean:**	**22.70**				
	Std. Dev.:	*0.10*				
3D6dIgA5C5a	**Mean:**	**24.84**	**0.22**			
	Std. Dev.:	*0.03*				
3D6dIgA5C5b	**Mean:**	**24.82**				
	Std. Dev.:	*0.03*				
3D6dIgA5C5c	**Mean:**	**24.78**				
	Std. Dev.:	*0.02*				

λ - Light Chain

DNA Isolate	Parameter	Cq-Value	ΔCq-Value	Efficiency 1/10	Efficiency LinReg	Efficiency Camper
4B3dIgA6H2a	**Mean:**	**21.39**	**-2.71**	**1.92**	**2.11**	**1.97**
	Std. Dev.:	*0.21*				
4B3dIgA6H2b	**Mean:**	**21.59**				
	Std. Dev.:	*0.19*				
4B3dIgA6H2c	**Mean:**	**21.54**				
	Std. Dev.:	*0.14*				

κ - Light Chain						
DNA Isolate	**Parameter**	**Cq-Value**	**∆Cq-Value**	**Efficiency 1/10**	**Efficiency LinReg**	**Efficiency Camper**
3D6dIgA5C5a	**Mean:**	**24.88**	**0.31**	**1.98**	**2.05**	**2.01**
	Std. Dev.:	*0.13*				
3D6dIgA5C5b	**Mean:**	**24.92**				
	Std. Dev.:	*0.14*				
3D6dIgA5C5c	**Mean:**	**24.91**				
	Std. Dev.:	*0.09*				

5.4.3 Quantification

The obtained Cq values and the mean efficiencies of each amplicon group were then used for the different quantification methods. Table 19 shows the relative gene copy results from the different quantification methods.

Table 19: Relative Quantifications:

Heavy Chain					
		ratio ($E^{\Delta Cq}$) for:			
	Parameter	**E (2)**	**E (1/10 method)**	**E (LinReg)**	**E (Camper)**
4B3dIgA6H2	**Mean:**	**4.35**	**6.37**	**16.37**	**10.29**
	Std. Dev.:	*0.76*	*0.67*	*1.86*	*1.08*
3D6dIgA5C5	**Mean:**	**2.05**	**3.15**	**8.26**	**5.21**
	Std. Dev.:	*0.24*	*0.5*	*1.14*	*0.68*

		ratio ($E^{\Delta\Delta Cq}$) for:			
	Parameter	**E (2)**	**E (1/10 method)**	**E (LinReg)**	**E (Camper)**
3D6/4B3	**Mean:**	**0.47**	**0.49**	**0.49**	**0.51**
	Std. Dev.:	*0.1*	*0.09*	*0.09*	*0.08*

Joining Chain					
		ratio ($E^{\Delta Cq}$) for:			
	Parameter	**E (2)**	**E (1/10 method)**	**E (LinReg)**	**E (Camper)**
4B3dIgA6H2	**Mean:**	**2.72**	**3.47**	**11.21**	**6.47**
	Std. Dev.:	*0.1*	*0.35*	*1.21*	*0.66*
3D6dIgA5C5	**Mean:**	**0.86**	**1.16**	**3.81**	**2.27**
	Std. Dev.:	*0.04*	*0.12*	*0.42*	*0.24*

		ratio ($E^{\Delta\Delta Cq}$) for:			
	Parameter	**E (2)**	**E (1/10 method)**	**E (LinReg)**	**E (Camper)**
	Mean:	**0.32**	**0.34**	**0.34**	**0.35**
3D6/4B3	*Std. Dev.:*	*0.02*	*0.05*	*0.05*	*0.05*

Light Chain

		(ratio $E^{\Delta Cq}$) for:			
	Parameter	**E (2)**	**E (1/10 method)**	**E (LinReg)**	**E (Camper)**
	Mean:	**6.58**	**9.75**	**4.44**	**6.59**
4B3dIgA6H2	*Std. Dev.:*	*0.86*	*1.42*	*0.73*	*0.99*
	Mean:	**0.81**	**0.64**	**0.98**	**0.55**
3D6dIgA5C5	*Std. Dev.:*	*0.05*	*0.08*	*0.14*	*0.07*

		ratio ($E^{\Delta\Delta Cq}$) for:			
	Parameter	**E (2)**	**E (1/10 method)**	**E (LinReg)**	**E (Camper)**
	Mean:	**0.12**	**0.07**	**0.22**	**0.08**
3D6/4B3	*Std. Dev.:*	*0.02*	*0.01*	*0.05*	*0.02*

The numeric results are depicted in the figures below (Figure 27 - Figure 29). Every quantification method gave different values. The pattern of relative gene copies of 4B3-IgA/6H2 looked different for each method used (see Figure 27) whereas for 3D6-IgA/5C5 the pattern was quite similar, HC was higher than JC than LC (Figure 28).

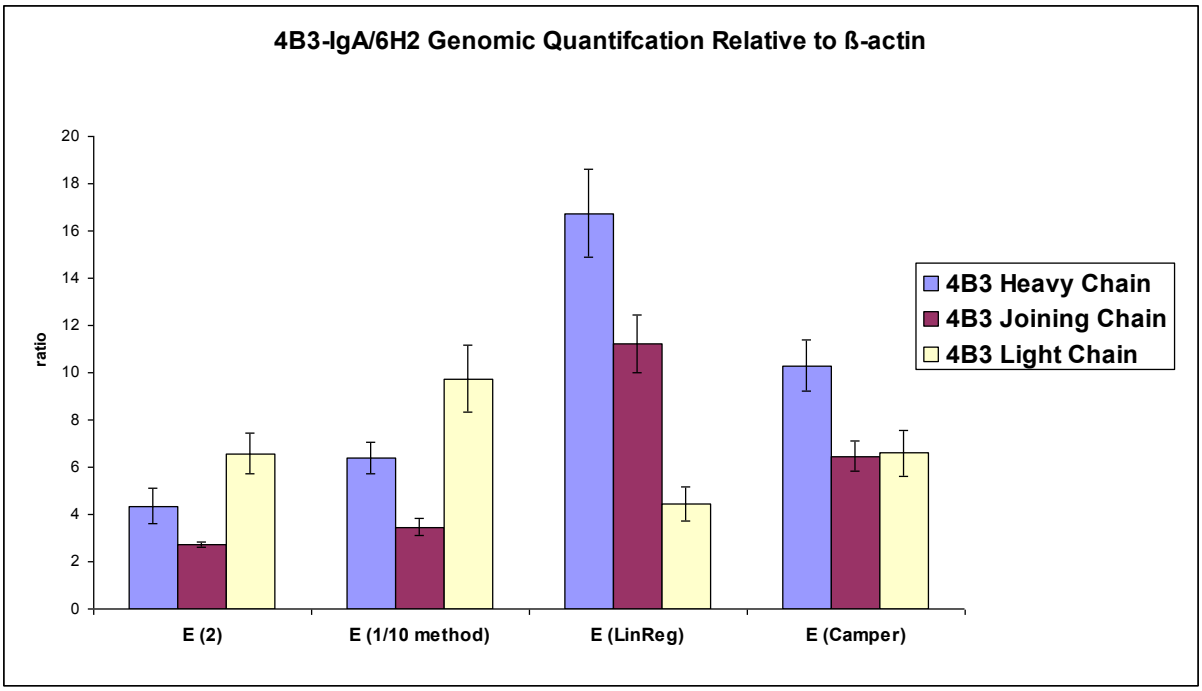

Figure 27: 4B3-IgA/6H2 quantifications relative to ß-actin.

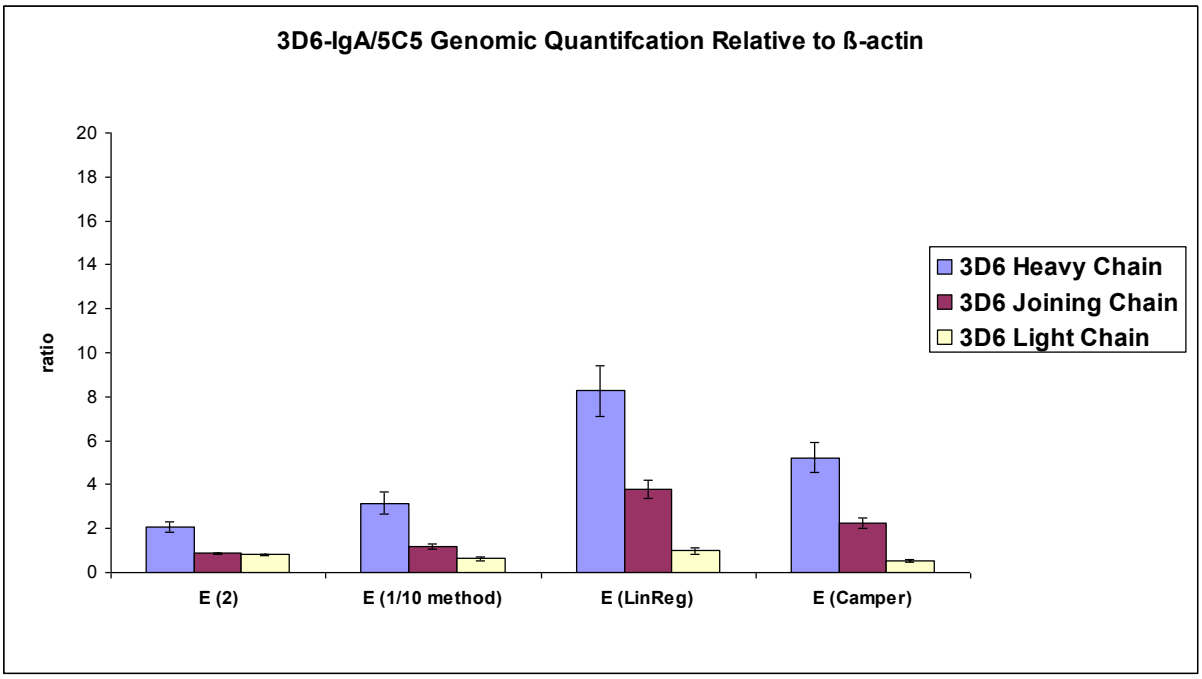

Figure 28:3D6-IgA/5C5 quantifications relative to ß-actin.

In Figure 29 3D6-IgA/5C5 is related to 4B3-IgA/6H2. However the obtained relations between the two cell lines were surprisingly similar for all used methods. In terms of HC 3D6 had half the gene copies of 4B3 whereas in terms of JC it was a third and

the relation of LC lied between ¼ and 1/10. The applied quantification methods showed very similar results, except the bigger variation of the LC ratios.

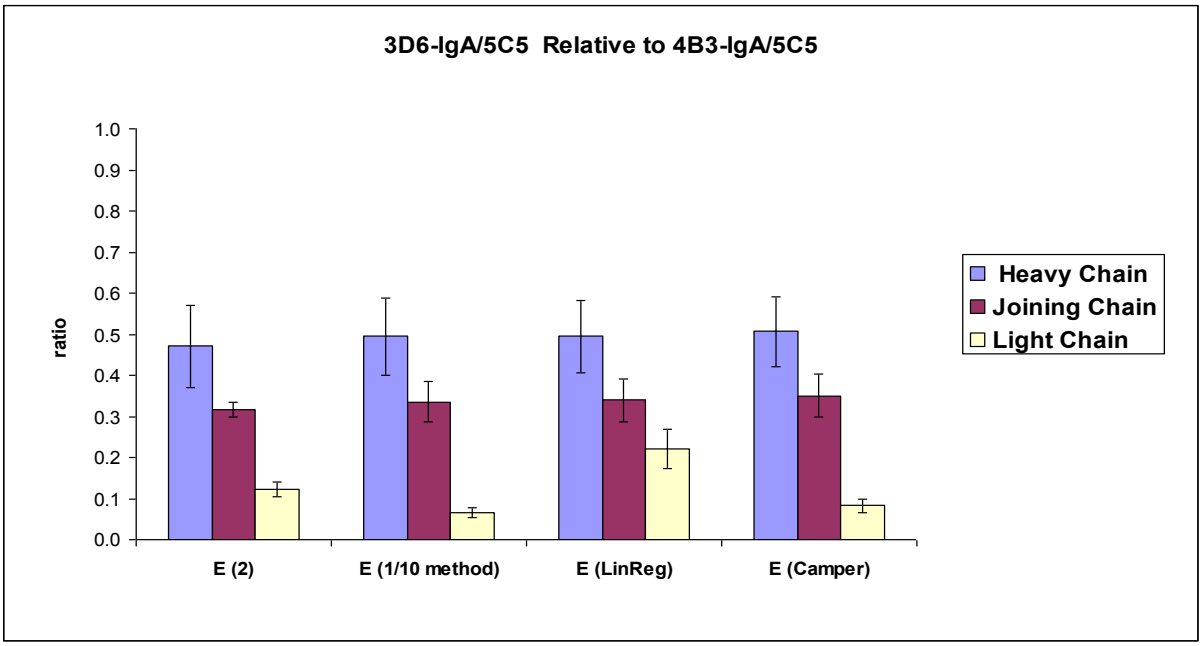

Figure 29: Genomic Differences between 3D6-IgA/5C5 and 4B3-IgA/6H2

The aim of this work was to evaluate qPCR quantification methods and their applicability for evaluation of recombinant cell lines. The obtained results showed that every applied relative quantification method gave different relative gene copy numbers. The ratio of HC and JC of the two compared cell lines was very similar for different efficiency calculation methods. For HC and JC the amplicon was the same and therefore the efficiency got cut out of the formula that was used to calculate the ratio between two samples (Figure 17). In terms of LC two different amplicons (lambda and kappa chains specific amplicons) were detected by qPCR and therefore the different efficiency calculations had a significant impact on the ratio that related 3D6-IgA/5C5 to 4B3-IgA/6H2. Therefore the choice of the efficient calculation was essential.

5.5 Transcript Copy Analysis

The mRNA was isolated from the different cell lines, reverse transcribed and analysed with real-time PCR as described in the methods part. The sample specific Cq values of each gene of interest was analysed using $2^{-\Delta\Delta Cq}$ method as well as the Pfaffl – method. The efficiencies for the Pfaffl – method were calculated with the 1/10 dilution method as well as mathematical algorithms using the LinReg and Camper software applications.

5.5.1 Raw Data

The mean Cq values, ΔCq values and the differently calculated efficiencies of the triplicates measured in two PCR runs for each GOI of all generated cDNAs, are listed in the table below:

Table 20: Table summarizes the Cq raw data, ΔCq-Values and efficiencies generated by different methods from the three biological replicates of the two production clones.

ß-actin						
RNA Isolate	**Parameter**	**Cq-Value**	**ΔCq-Value**	**Efficiency 1/10**	**Efficiency LinReg**	**Efficiency Camper**
4B3dIgA6H2a	**Mean:**	**18.26**	**Reference**	**1.98**	**2.03**	**2.01**
	St. Dev.:	*0.07*				
4B3dIgA6H2b	**Mean:**	**17.96**				
	St. Dev.:	*0.10*				
4B3dIgA6H2c	**Mean:**	**18.84**				
	St. Dev.:	*0.06*				
3D6dIgA5C5a	**Mean:**	**18.37**	**Reference**			
	St. Dev.:	*0.11*				
3D6dIgA5C5b	**Mean:**	**18.15**				
	St. Dev.:	*0.08*				
3D6dIgA5C5c	**Mean:**	**19.05**				
	St. Dev.:	*0.13*				

Heavy Chain

RNA Isolate	Parameter	Cq-Value:	ΔCq-Value	Efficiency 1/10	Efficiency LinReg	Efficiency Camper
4B3dIgA6H2a	**Mean:**	**22.64**	**4.20**	**1.91**	**1.91**	**1.88**
	St. Dev.:	*0.18*				
4B3dIgA6H2b	**Mean:**	**21.80**				
	St. Dev.:	*0.16*				
4B3dIgA6H2c	**Mean:**	**23.21**				
	St. Dev.:	*0.12*				
3D6dIgA5C5a	**Mean:**	**21.90**	**3.26**			
	St. Dev.:	*0.10*				
3D6dIgA5C5b	**Mean:**	**21.13**				
	St. Dev.:	*0.05*				
3D6dIgA5C5c	**Mean:**	**22.31**				
	St. Dev.:	*0.17*				

Joining Chain

RNA Isolate	Parameter	Cq-Value:	ΔCq-Value	Efficiency 1/10	Efficiency LinReg	Efficiency Camper
4B3dIgA6H2a	**Mean:**	**24.51**	**6.15**	**1.89**	**1.82**	**1.87**
	St. Dev.:	*0.19*				
4B3dIgA6H2b	**Mean:**	**24.07**				
	St. Dev.:	*0.12*				
4B3dIgA6H2c	**Mean:**	**24.93**				
	St. Dev.:	*0.17*				
3D6dIgA5C5a	**Mean:**	**24.51**	**5.97**			
	St. Dev.:	*0.23*				
3D6dIgA5C5b	**Mean:**	**24.03**				
	St. Dev.:	*0.11*				
3D6dIgA5C5c	**Mean:**	**24.94**				
	St. Dev.:	*0.15*				

λ - Light Chain

RNA Isolate	Parameter	Cq-Value:	ΔCq-Value	Efficiency 1/10	Efficiency LinReg	Efficiency Camper
4B3dIgA6H2a	**Mean:**	**19.10**	**0.78**	**1.95**	**1.92**	**1.95**
	St. Dev.:	*0.23*				
4B3dIgA6H2b	**Mean:**	**18.49**				
	St. Dev.:	*0.48*				
4B3dIgA6H2c	**Mean:**	**19.82**				
	St. Dev.:	*0.18*				

κ - Light Chain						
RNA Isolate	**Parameter**	**Cq-Value:**	**ΔCq-Value**	**Efficiency 1/10**	**Efficiency LinReg**	**Efficiency Camper**
3D6dIgA5C5a	**Mean:**	**20.00**	**1.73**	**1.91**	**1.88**	**1.85**
	St. Dev.:	*0.20*				
3D6dIgA5C5b	**Mean:**	**20.02**				
	St. Dev.:	*0.15*				
3D6dIgA5C5c	**Mean:**	**20.75**				
	St. Dev.:	*0.00*				

5.5.2 Quantification

The obtained Cq values and the mean efficiencies of each amplicon group of the analysed cDNA were then used for the different quantification methods. The results are shown in Table 21.

Table 21: Quantification using the different methods.

Heavy Chain					
		ratio ($E^{\Delta Cq}$) for:			
	Parameter	**E (2)**	**E (1/10 method)**	**E (LinReg)**	**E (Camper)**
4B3dIgA6H2	**Mean:**	**0.06**	**0.13**	**0.2**	**0.24**
	Std. Dev.:	*0.01*	*0.01*	*0.02*	*0.03*
3D6dIgA5C5	**Mean:**	**0.11**	**0.24**	**0.38**	**0.45**
	Std. Dev.:	*0.02*	*0.03*	*0.04*	*0.04*

		ratio ($E^{\Delta\Delta Cq}$) for:			
	Parameter	**E (2)**	**E (1/10 method)**	**E (LinReg)**	**E (Camper)**
3D6/4B3	**Mean:**	**1.91**	**1.85**	**1.86**	**1.83**
	Std. Dev.:	*0.57*	*0.31*	*0.28*	*0.27*

Joining Chain					
		ratio ($E^{\Delta Cq}$) for:			
	Parameter	**E (2)**	**E (1/10 method)**	**E (LinReg)**	**E (Camper)**
4B3dIgA6H2	**Mean:**	**0.01**	**0.05**	**0.19**	**0.08**
	Std. Dev.:	*0*	*0.01*	*0.02*	*0.01*
3D6dIgA5C5	**Mean:**	**0.02**	**0.05**	**0.22**	**0.09**
	Std. Dev.:	*0*	*0.01*	*0.03*	*0.01*

		ratio ($E^{\Delta\Delta Cq}$) for:			
	Parameter	**E (2)**	**E (1/10 method)**	**E (LinReg)**	**E (Camper)**
3D6/4B3	**Mean:**	**1.13**	**1.13**	**1.14**	**1.13**
	Std. Dev.:	*0.13*	*0.19*	*0.19*	*0.19*

Light Chain

		(ratio $E^{\Delta Cq}$) for:			
	Parameter	**E (2)**	**E (1/10 method)**	**E (LinReg)**	**E (Camper)**
4B3dIgA6H2	**Mean:**	**0.59**	**0.8**	**1.65**	**0.95**
	Std. Dev.:	*0.1*	*0.17*	*0.34*	*0.21*
3D6dIgA5C5	**Mean:**	**0.3**	**0.63**	**1.32**	**1.59**
	Std. Dev.:	*0.03*	*0.09*	*0.19*	*0.22*

		ratio ($E^{\Delta\Delta Cq}$) for:			
	Parameter	**E (2)**	**E (1/10 method)**	**E (LinReg)**	**E (Camper)**
3D6/4B3	**Mean:**	**0.51**	**0.8**	**0.8**	**1.67**
	Std. Dev.:	*0.1*	*0.21*	*0.2*	*0.43*

In the table above the relative transcript copy numbers are listed according to the different quantification method. The numeric results are depicted in the figures below (Figure 30 - Figure 32). Every quantification method gave different values as also seen before with gDNA. The pattern of relative transcript copies of both clones looked similar for each method used (Figure 30, Figure 31). Both recombinant cell lines had more LC than HC than JC transcripts.

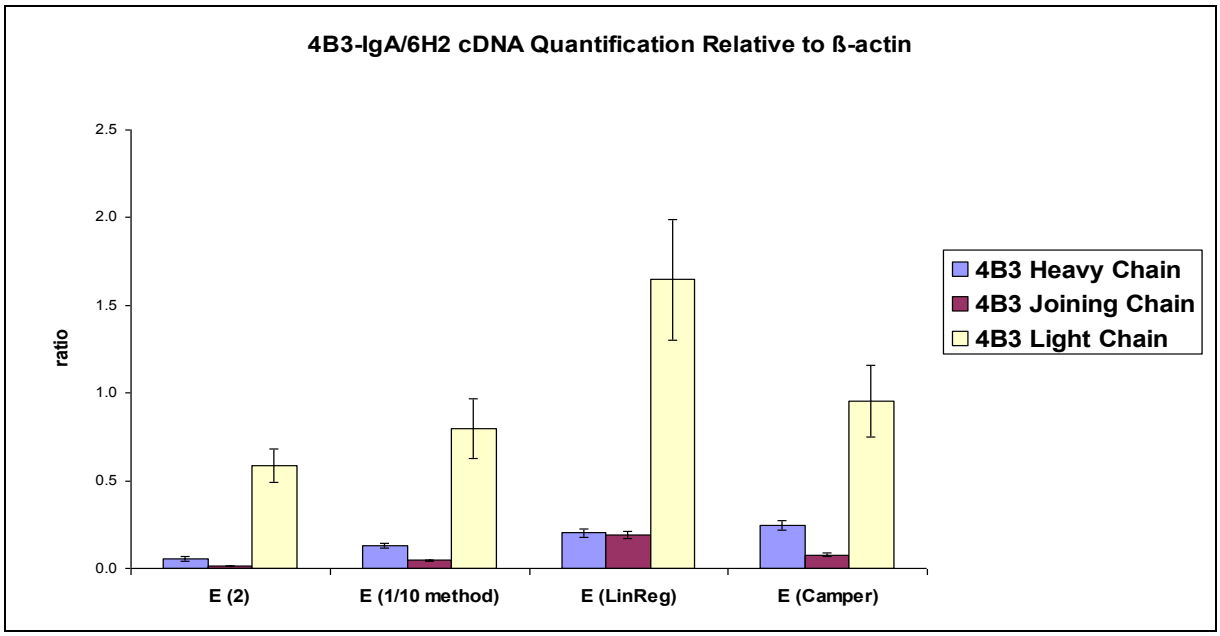

Figure 30: 4B3-IgA/6H2 quantification relative to ß-actin.

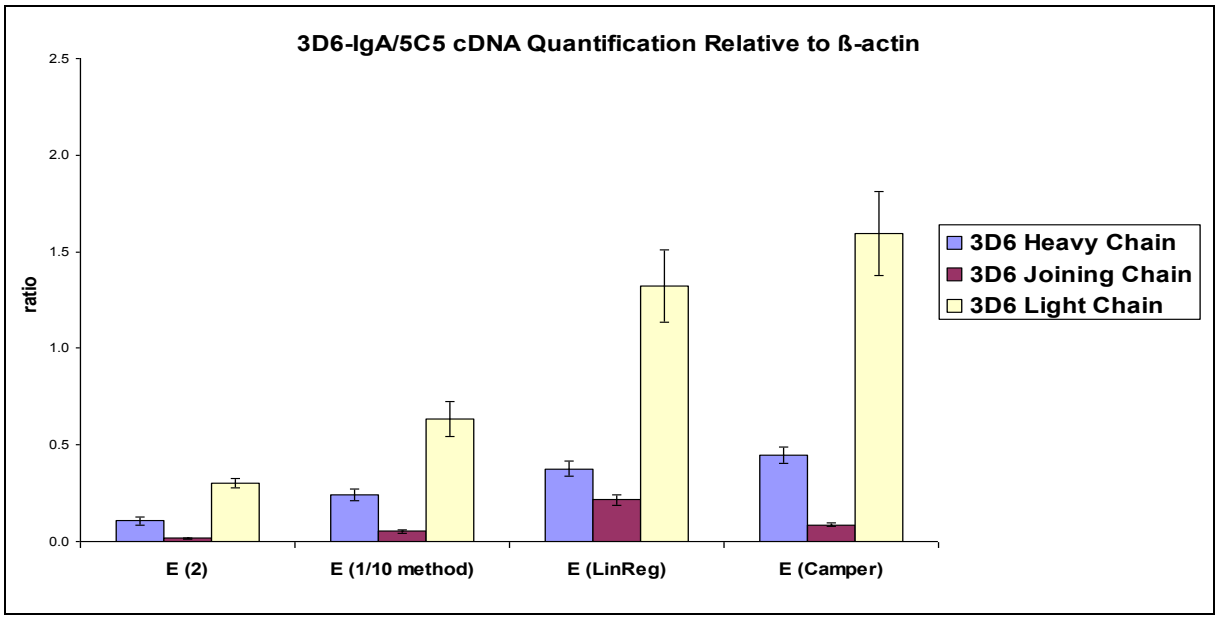

Figure 31: 3D6-IgA/5C5 quantification relative to ß-actin.

In Figure 32 the relation between 3D6-IgA/5C5 and 4B3-IgA/6H2 is depicted. 3D6 had twice the amount of HC and almost the same amount of JC transcripts compared to 4B3, the relation of LC lied between twice the amount and half the amount and therefore differed significantly between the used methods. We assumed that it was rather difficult to compare light chains of the two antibodies, since it was necessary to test them with different primers and probes, one specific for lambda and one specific for kappa light chain. Comparable to the genomic DNA the different methods gave similar results when comparing two cell lines.

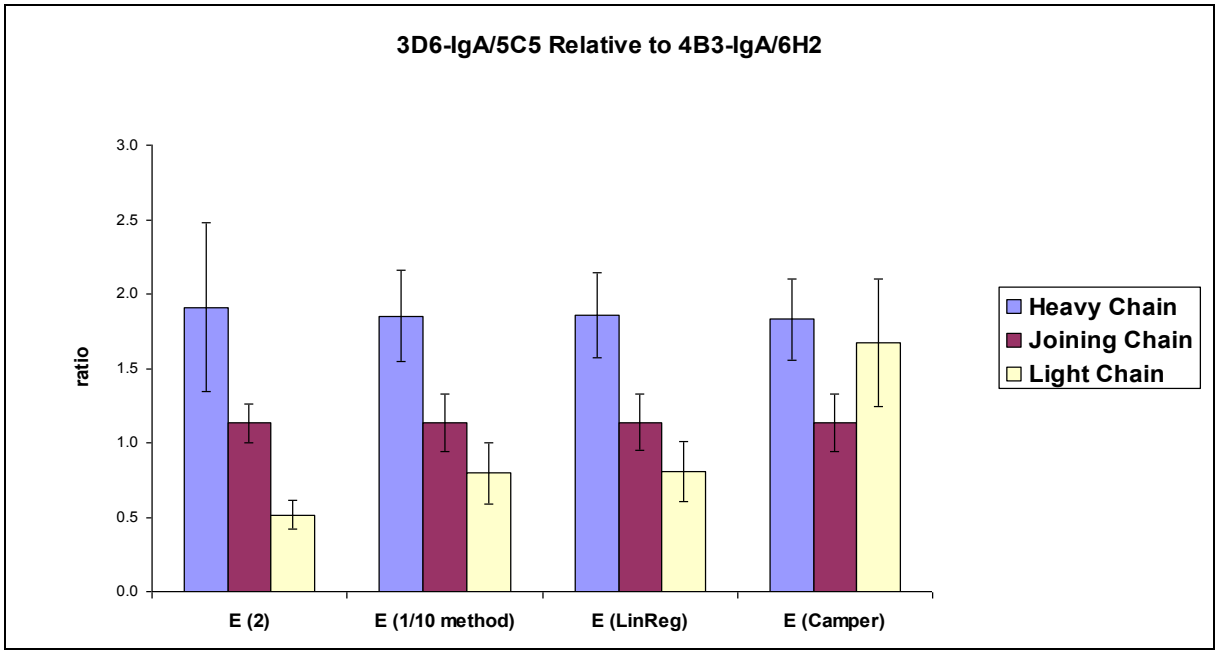

Figure 32: 3D6-IgA/5C5 relative to 4B3-IgA/6H2

5.6 Comparison of gDNA and cDNA Content

On the previous pages several methods for quantification were compared, because of the repeatability and the practical usability I chose the relative quantification using the LinReg software application for efficiency correction for further comparisons.

In Figure 33 the relative gene copies and the relative amount of transcripts relative to ß-actin are presented.

Regarding to the number of gene copies of all of the genes of interest 4B3-IgA/6H2 had more copies than 3D6-IgA/5C5 but the relations between the 3 different chains were quite similar for both recombinant cell lines. 4B3-IgA/6H2 had about twice the amount of HC, about 3 times the amount of JC and about 4 times the amount of LC genes integrated in the genome compared to 3D6-IgA/5C5.

Regarding the amount of GOI transcripts there was no big difference obtained between the two recombinant cell lines. According to LC and JC no significant difference could be identified. In terms of heavy chain 3D6-IgA/5C5 had approximately double the amount of transcripts meaning that transcription was four times more efficient. Both recombinant cell lines have more LC transcripts than JC and HC.

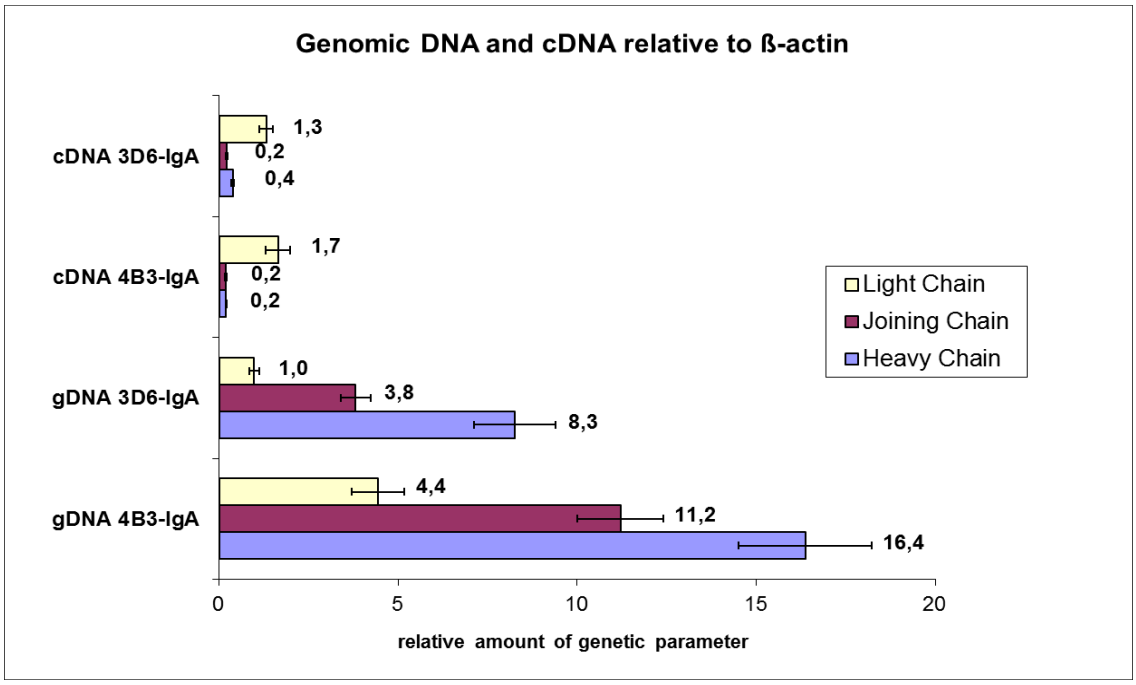

Figure 33: Comparison of the different genes of interest in genomic DNA and cDNA relative to ß-actin calculated with the mean delta Cq values and the mean LinReg efficiencies for efficiency correction.

5.7 Product Purification

IgA from both recombinant cell lines 4B3-IgA/6H2 and 3D6-IgA/5C5 was affinity purified from concentrated culture supernatants using an Äkta purifier and CaptureSelect human IgA as stationary phase material. Figure 34 shows a typical chromatogram of the applied purification scheme.

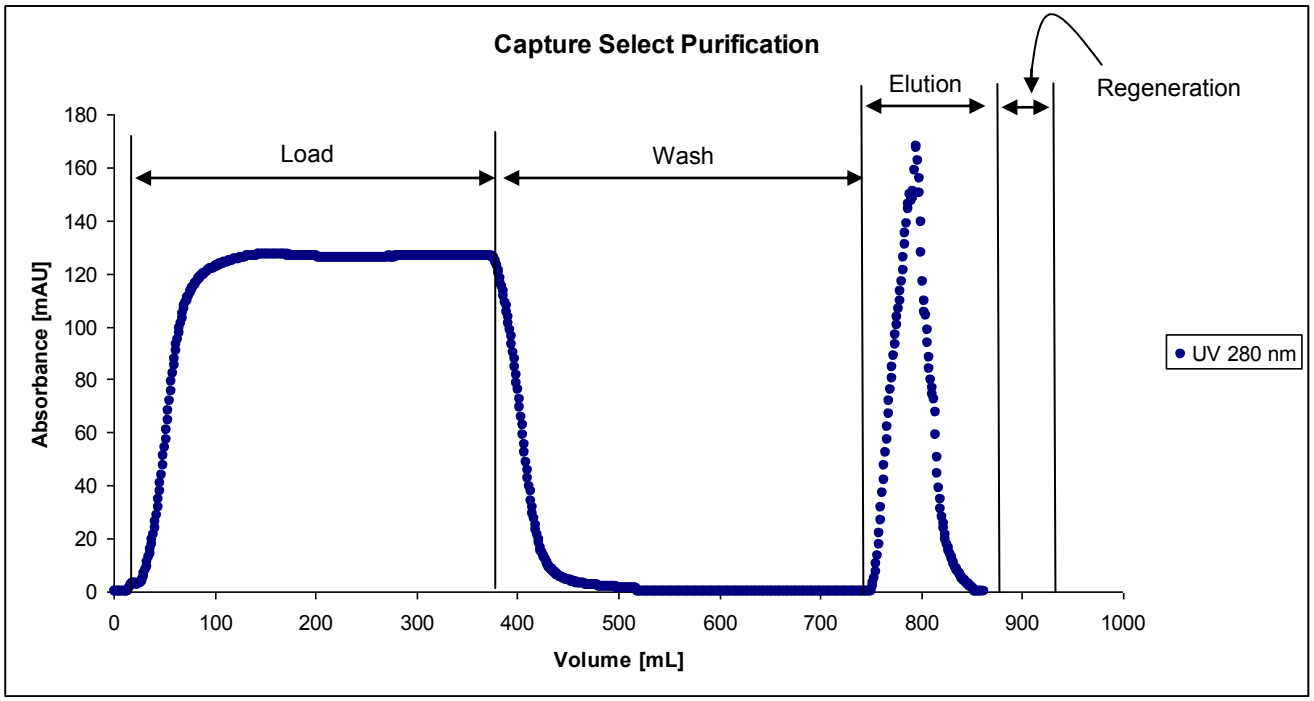

Figure 34: Example Chromatogram of one capture select purification.

Fractions eluted during chromatography were electrophoretically separated by SDS-PAGE and subsequently analysed by silver staining. Figure 35 shows the obtained gel fractions after chromatography of 4B3-IgA and 3D6-IgA samples. High amounts of impurities were present in the load, flow-through and wash fractions in both 4B3-IgA and 3D6-IgA purification experiments. Also, both regeneration fractions contained only minimal amounts of protein. Monomeric IgA has a molecular weight of ~160 kDa. Dimeric IgA connected with the Joining chain has a theoretical molecular weight of about 335 kDa. The elution fraction of 4B3-IgA showed a single band migrating as expexted for a dimeric IgA molecule. This band indicated dIgAs of 4B3 specificity. In the 3D6-IgA elution fraction three product bands were visible. The band running at approximately 160 kDa was monomeric IgA, the band in the middle

represented dimeric IgA linked with JC. The high molecular weight band that migrated above the 460 kDa marker was a mixture of oligomeric IgAs.

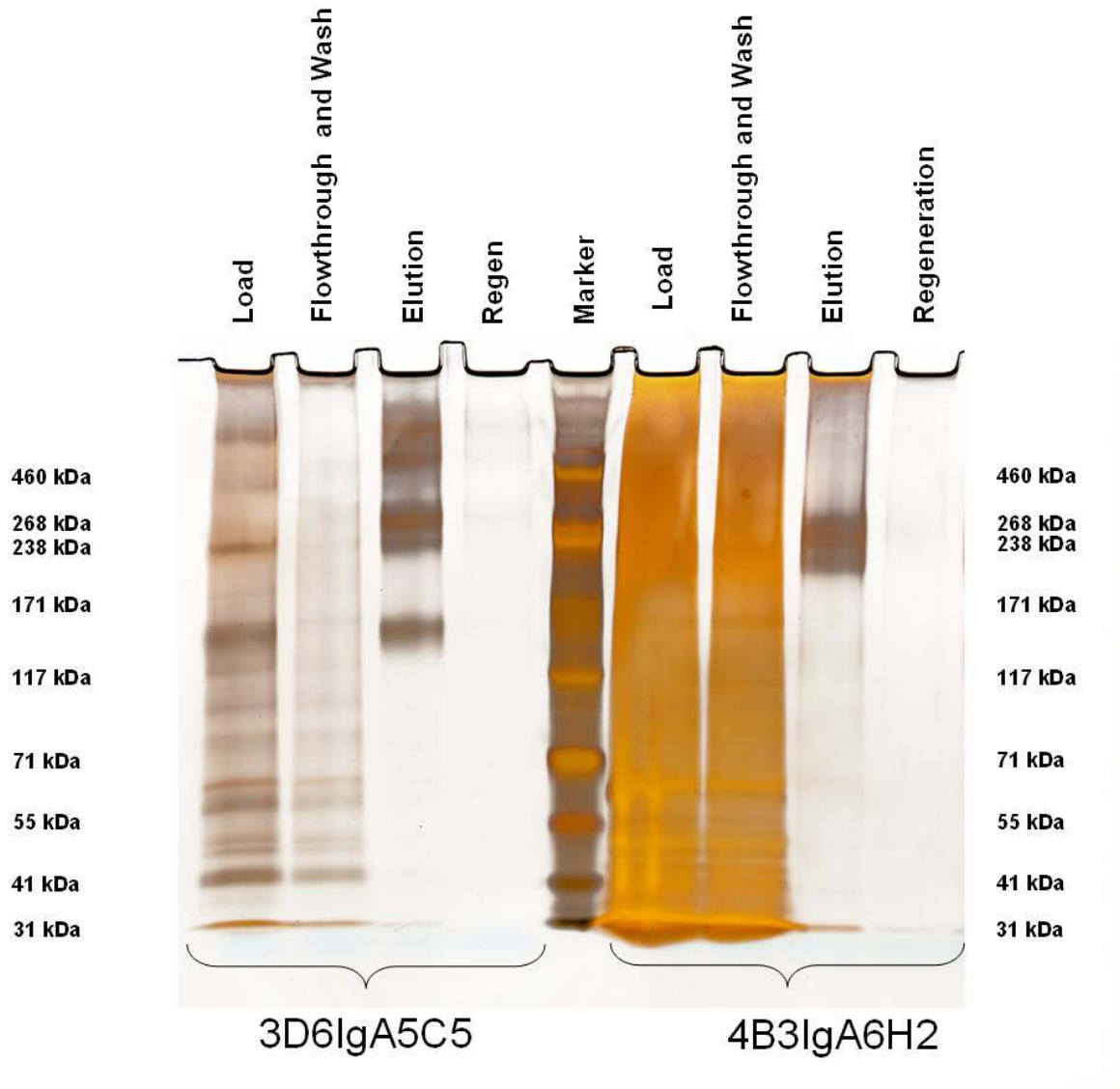

Figure 35: Polyacrylamide gel, silver stained showing the different fractions of one 3D6-IgA and one 4B3-IgA purification.

The recovery rate of product in the elution fraction was > 90 %. IgAs were confirmed by western blot (data not shown).

6 Discussion

6.3 Growth and Productivity

The two recombinant cell lines were propagated and observed over 41 passages (~ 144 days) to compare their growth rates and productivities. Significant differences in IgA specific productivity were identified. Clone 3D6-IgA/5C5 secreted almost 80-fold more product than clone 4B3-IgA/6H2 (Figure 25) although the set of plasmids used for the CHO host cell transfection was similar for both recombinant clones.

The growth rate and specific productivity of clone 3D6-IgA/5C5 had a slightly positive trend over the whole cultivation time. Clone 4B3-IgA/6H2 had an increase of growth rate but a decrease in productivity at the end of the propagation. The phenomenon of loss of productivity was attributed to the fact that higher producers normally grow slower than low or non-producing cells and can therefore overgrow a high-producing cell population. However, 4B3-IgA/6H2 was considered to be stable till passage 48 (Figure 21).

The mean growth rates over time of both recombinant IgA producing cell lines 4B3-IgA/6H2 and 3D6-IgA/5C5 were similar to the CHO host cell line (Figure 23). Clone 3D6-IgA/5C5 had the highest growth rate followed by the host cell line and clone 4B3-IgA/6H2. This result was not expected, since producers generally grow slower than non–producing cell lines. This observation may be attributable to the different cultivation vessels and media. Both recombinant cell lines were always passaged to a starting cell density of $2.5x10^5$ cells per mL and reached relatively high cell densities. 3D6-IgA/5C5 reached maximal cell densities of ~$3.5x10^6$ cells whereas 4B3-IgA/6H2 reached a maximum of ~$2.3x10^6$ cells per mL. The host cell line that was passaged to a starting cell density of $2x10^5$ cells per mL in T-flask reached maximal cell densities of ~$1.5x10^6$ cells per mL. Another point to consider is the cell metabolism. The dhfr negative host cell line needs to generate nucleotides via the salvage pathway, while the producer cells were transfected with dhfr and selected for stable expression of dhfr and therefore nucleotides can be generated by de novo synthesis.

6.4 Cell Line Characterization via qPCR

The aim of this project was to investigate potential reasons for the observed differences in IgA productivity of the recombinant cell lines. As described in the introduction part one explanation could be a difference in gene copies or transcription rates of one or more genes of interest. To find out if there were differences on the genetic or transcript level real-time PCR was performed.

6.4.1 Genomic DNA pre-Denaturation improves qPCR Results

As depicted in Figure 26 pre-denatured genomic DNA data was less noisy and had a more precise distribution of curves in a multi-parallel experiment. This phenomenon was discovered before (*25*) for another PCR machine and was attributed to a slight temperature variance for each reaction mix inside the qPCR machine. This temperature heterogeneity could cause incomplete denaturation in some wells during the first denaturation step of the qPCR and therefore led to less free template DNA in the first few cycles. My observation approved the advantage of genomic DNA pre-denaturation to obtain more precise and less scattered data.

6.4.2 The Challenge of qPCR Data Interpretation

Real-time PCR is a very sensitive and progressive method and routinely and widely used in research but there is still no standardized quantification or efficiency calculation method available. Although relative quantification methods seem to be the most progressive ones, there is still research published containing data that was quantified absolutely what makes it sometimes hard to compare obtained results with others found in literature. Nowadays everyone does quantifications in a different way what lowers the expressiveness of qPCR obtained data.

Several methods to quantify the initial template concentration of specific genes are described in literature. Relative quantification using an internal reference gene is a

widely used method and appeared most progressive. Among these is the $2^{-\Delta\Delta Cq}$ method that was first described by Livak et al. (*22*) and assumes 100% amplification efficiencies indicated by a doubling of the specific gene after each PCR cycle. Pfaffl et al. (*23*) modified and improved the method by considering the individual efficiency of the PCR run. This new quantification strategy seems to be the most accurate method for qPCR quantification but opens the question of how to calculate the PCR efficiency.

As described in the methods part there are in principal two ways of efficiency calculation. One way is based on a 1/10 dilution series whereas the other way is based on mathematical algorithms that calculate the efficiency from the relative fluorescence units curve itself.

The drawback of the 1/10 method is that a 1/10 dilution series is error-prone because of the operator error while pipetting. Furthermore it is a time and material consuming way to obtain the qPCR efficiency and during my practical work I experienced bad repeatability of efficiencies with this method although the sample Cq values were not differing among different qPCR runs.

The other way of efficiency determination is based on mathematical algorithms. In this project the two applications LinReg and Camper were used for deeper comparison with the other methods. In common the reproducibility of efficiencies received from this software applications were good and the mean efficiency values were mostly comparable to the mean ones obtained from the 1/10 method.

Nevertheless, small changes in efficiency values can cause huge differences in relative quantification what is understandable in regard to the formulas that are used for calculations (Figure 17). For this reason every efficiency calculation method led to diverse values of relative differences to ß-actin. Nonetheless, the values of the comparisons between the two recombinant cell lines were quite similar for all methods.

The LinReg software application for efficiency correction was reproducible, easy to handle, practically usable due to the free software access and due to the fact that no pipetting error sophisticates the efficiency calculation results. For further discussion of our clones we used results gained by the LinReg method.

6.4.3 Gene Copies and Transcript Copies versus Specific Productivity

The gene copy number of all IgA related genes was in the range between 1 and 16 fold compared to ß-actin, with the lowest value for 3D6-IgA/5C5 LC which was only 30 % higher then ß-actin (Table 21).

Both recombinant cell lines had more HC than JC than LC genes. The higher amount of HC genes for both cell lines is maybe attributable to the fact that the dhfr- gene was provided by the same plasmid as the HC and therefore higher co-amplified than the other genes of interest by the addition of MTX. Furthermore the amount of LC was for both cell lines the lowest what may be attributable to the fact that the LC transfection plasmid had no selection marker.

By analysing the cDNA resulting from RNA transcripts we found that the transgenes were not at all transcribed with the same efficacy. Although 4B3-IgA/6H2 had in general 2 – 4 times higher GCNs than 3D6-IgA/5C5, the amount of transcripts was similar for both clones. In terms of heavy chain transcripts the obtained amount in 4B3-IgA/6H2 was only half of the amount obtained for 3D6-IgA/5C5. This observation is probably referred to the integration locus in the genome. It is well known that chromatin structure and therefore the locus of integration into the genome can be crucial for proper transcription (*26*). For this reason a high gene copy number alone does not automatically lead to high amount of transcripts or productivities.

In contrast the LCs with low GCNs were identified to be transcribed with much higher efficiency leading to higher transcript amounts than ß-actin.

Table 22: Genetic paramters related to ß-actin (see Figure 33)

	Genetic Parameters related to β-actin			
	β-actin	HC	LC	JC
3D6-IgA/5C5 GCN	1.0	8.3	1.0	3.8
4B3-IgA/6H2 GCN	1.0	16.4	4.4	11.2
3D6-IgA/5C5 transcript amount	1.0	0.4	1.3	0.2
4B3-IgA/6H2 transcript amount	1.0	0.2	1.7	0.2

We also tried to take transcript amount into account for protein expression: The JCs showed also reduced transcription efficiency compared to LCs, but the influence on product formation could not be estimated since dIgAs consist of 4 heavy chains and light chain combined with only one JC and consequently JC does not seem to be the limiting factor for dIgA expression. This view suggested that HC was the limiting transcript for IgA expression. However, the results summarized in table 22 gave us additional and somehow controversial information. If HC was the limiting factor for protein expression we would assume that 3D6-IgA/5C5 and 4B3-IgA/6H2 express similar amounts or 3D6-IgA/5C5 could express a two fold increase of 4B3-IgA/6H2. In reality we found that 3D6-IgA/5C5 expressed 80 fold more IgA than 4B3-IgA/6H2, and as already assumed from previous antibodies (personal communication), the amount of transcript is not the limiting factor in this case.

Table 23: Specific productivity compared to the amount of transcript.

Specific productivity qp	[µg/d*10^6 cells]			
3D6-IgA/5C5	3.75			
4B3-IgA/6H2	0.05			
Transcript amount relative to ß-actin	β-actin	HC	LC	JC
3D6-IgA/5C5	1.0	0.4	1.3	0.2
4B3-IgA/6H2	1.0	0.2	1.7	0.2

6.5 Product Purification

IgA purification using the CaptureSelect human IgA matrix is a robust and well-performing method. The advantage of this method compared to others is that the product can be purified in one step. Although the protein content of the load fraction was high for both cell lines' supernatant concentrates, the eluate fraction contained just highly purified IgA. 4B3-IgA/6H2 mainly formed dimeric IgA whereas 3D6-IgA/5C5 also produced a large amount of monomers and higher oligomers. In summary, the IgA purification protocol described by Reinhart et al. (*11*) was repeatable and therefore a good choice for IgA purification.

7 Conclusion

There is a big difference between the two recombinant cell lines 4B3-IgA/6H2 and 3D6-IgA/5C5 according to their productivities although both cells were transfected with a similar set of genetic information.

The proposal of my work was to analyse the difference of the two production cell lines according to the genes of interest on the genome or transcript level. Together with the product secretion level we evaluated the influence of gene copy transcription efficiency and translation capacity of the individual clones expressing two different IgAs. We found that gene copy numbers between the two clones differed with a maximum factor of 4 but corresponding amounts of specific transcripts could not be correlated to gene copy numbers. Nevertheless, the amount of specific transcripts was similar for both clones indicated by a maximal factor of two. However the productivity of the 3D6-IgA expressing cell line was approximately 80-fold higher than the productivity of 4B3-IgA.

This led to the hypothesis that there was either a translational or protein folding problem or a bottleneck in the secretion pathway of 4B3-IgA despite the antibody did not obviously contain unnatural mutations or structures.

Both antibodies were produced in recombinant cell lines and an IgA affinity purification using camelid ligands (*11*) was used to purify milligram amounts of both proteins.

8 References

1. F. M. Wurm, Production of recombinant protein therapeutics in cultivated mammalian cells. *Nat Biotechnol* **22**, 1393 (Nov, 2004).
2. G. Urlaub, L. A. Chasin, Isolation of Chinese hamster cell mutants deficient in dihydrofolate reductase activity. *Proc Natl Acad Sci U S A* **77**, 4216 (Jul, 1980).
3. J. Chusainow *et al.*, A study of monoclonal antibody-producing CHO cell lines: what makes a stable high producer? *Biotechnol Bioeng* **102**, 1182 (Mar, 2009).
4. C. Lattenmayer *et al.*, Characterisation of recombinant CHO cell lines by investigation of protein productivities and genetic parameters. *J Biotechnol* **128**, 716 (Mar, 2007).
5. G. Walsh, Biopharmaceuticals: recent approvals and likely directions. *Trends Biotechnol* **23**, 553 (Nov, 2005).
6. H. W. Schroeder, L. Cavacini, Structure and function of immunoglobulins. *J Allergy Clin Immunol* **125**, S41 (Feb, 2010).
7. J. G. Elvin, R. G. Couston, C. F. van der Walle, Therapeutic antibodies: Market considerations, disease targets and bioprocessing. *Int J Pharm*, (Dec, 2011).
8. J. M. Woof, M. A. Kerr, The function of immunoglobulin A in immunity. *J Pathol* **208**, 270 (Jan, 2006).
9. B. Corthésy, Recombinant immunoglobulin A: powerful tools for fundamental and applied research. *Trends Biotechnol* **20**, 65 (Feb, 2002).
10. W. Unaids. (Joint United Nations Programme on HIV/AIDS (UNAIDS), http://www.unaids.org/globalreport/Global_report.htm, 2010), pp. 360.
11. D. Reinhart, R. Weik, R. Kunert, Recombinant IgA production: Single step affinity purification using camelid ligands and product characterization. *Journal of Immunological Methods* **378**, 95 (2012).
12. D. Reinhart, R. Weik, R. Kunert, 3D6 and 4B3: Recombinant expression of two anti-gp41 antibodies as dimeric and secretory IgA. *BMC Proc* **5 Suppl 8**, P56 (Nov, 2011).
13. S. Rozen, H. Skaletsky, Primer3 on the WWW for general users and for biologist programmers. *Methods Mol Biol* **132**, 365 (2000).
14. W. A. Kibbe, OligoCalc: an online oligonucleotide properties calculator. *Nucleic Acids Res* **35**, W43 (Jul, 2007).
15. C. Ramakers, J. M. Ruijter, R. H. Deprez, A. F. Moorman, Assumption-free analysis of quantitative real-time polymerase chain reaction (PCR) data. *Neurosci Lett* **339**, 62 (Mar, 2003).
16. J. M. Ruijter *et al.*, Amplification efficiency: linking baseline and bias in the analysis of quantitative PCR data. *Nucleic Acids Res* **37**, e45 (Apr, 2009).
17. J. M. Tuomi, F. Voorbraak, D. L. Jones, J. M. Ruijter, Bias in the Cq value observed with hydrolysis probe based quantitative PCR can be corrected with the estimated PCR efficiency value. *Methods* **50**, 313 (Apr, 2010).
18. A. Tichopad, M. Dilger, G. Schwarz, M. W. Pfaffl, Standardized determination of real-time PCR efficiency from a single reaction set-up. *Nucleic Acids Res* **31**, e122 (Oct, 2003).
19. X. Xu *et al.*, The genomic sequence of the Chinese hamster ovary (CHO)-K1 cell line. *Nat Biotechnol* **29**, 735 (Aug, 2011).
20. S. A. Bustin *et al.*, The MIQE guidelines: minimum information for publication of quantitative real-time PCR experiments. *Clin Chem* **55**, 611 (Apr, 2009).
21. K. Doerffel, *Statistik in der analytischen Chemie*. (Dt. Verl. für Grundstoffindustrie, Leipzig, ed. 5., erw. und überarb. Aufl.. 1990), pp. 256 S.
22. K. J. Livak, T. D. Schmittgen, Analysis of relative gene expression data using real-time quantitative PCR and the 2(-Delta Delta C(T)) Method. *Methods* **25**, 402 (Dec, 2001).

23. M. W. Pfaffl, A new mathematical model for relative quantification in real-time RT-PCR. *Nucleic Acids Res* **29**, e45 (May, 2001).
24. S. A. Bustin, *A-Z of quantitative PCR*. IUL biotechnology series (International University Line, La Jolla, CA, 2009), pp. xxix, 882 p.
25. J. Wilhelm, M. Hahn, A. Pingoud, Influence of DNA target melting behavior on real-time PCR quantification. *Clin Chem* **46**, 1738 (Nov, 2000).
26. G. J. Narlikar, H. Y. Fan, R. E. Kingston, Cooperation between complexes that regulate chromatin structure and transcription. *Cell* **108**, 475 (Feb, 2002).

STATUTORY DECLARATION

I declare that I have authored this thesis independently, that I have not used other than the declared sources / resources, and that I have explicitly marked all material which has been quoted either literally or by content from the used sources.

Vienna, April 2012 Sommeregger Wolfgang

EIDESSTATTLICHE ERKLÄRUNG

Ich erkläre an Eides statt, dass ich die vorliegende Arbeit selbstständig verfasst, andere als die angegebenen Quellen/Hilfsmittel nicht benutzt, und die den benutzten Quellen wörtlich und inhaltlich entnommene Stellen als solche kenntlich gemacht habe.

Wien, April 2012 Sommeregger Wolfgang